의학박사 학위논문

산발성 불일치 복구 유전자 결핍 뇌종양 및 린치 증후군 관련 불일치 복구 유전자 결핍 뇌종양

Sporadic and Lynch syndrome-associated mismatch repair deficient brain tumors

2022년 8월

서울대학교 대학원

의학과 병리학전공

김 현 희

산발성 불일치 복구 유전자 결핍 뇌종양 및 린치 증후군 관련 불일치 복구 유전자 결핍 뇌종양

Sporadic and Lynch syndrome-associated mismatch repair deficient brain tumors

지도교수 박 성 혜

이 논문을 의학박사 학위논문으로 제출함

2022년 4월

서울대학교 대학원

의학과 병리학전공

김 현 희

김현희의 의학박사 학위논문을 인준함

2022년 7월

위 원 장 정 경 천 (인)

부위원장 박 성 혜 (인)

위 원 박 철 기 (인)

위 원 원 재 경 (인)

위 원 김 세 훈 (인)

Abstract

Sporadic and Lynch syndrome-associated mismatch repair deficient brain tumors

Hyunhee Kim

School of Medicine, Pathology Major

The Graduate School

Seoul National University

Mismatch repair-deficient (MMRD) brain tumors are rare among primary brain tumors and can be induced by germline or sporadic mutations.

Here, we report 25 MMRD-associated (21 sporadic and 4 Lynch syndrome) primary brain tumors to determine clinicopathological and molecular characteristics and biological behavior. Our 25 MMRD brain tumors included glioblastoma (GBM) IDH-wildtype (n = 17) including 1 gliosarcoma, astrocytoma IDH-mutant WHO grade 4 (n

= 3), diffuse midline glioma (DMG) H3 K27M-mutant (n = 1), anaplastic meningioma (n = 1), oligodendroglioma, IDH-mutant and 1p/19q-codeleted (n = 1), medulloblastoma with extensive nodularity, SHH-activated and TP53-wildtype WHO grade 4 (n = 1), and pleomorphic xanthoastrocytoma (PXA) (n = 1).

Next-generation sequencing using a brain tumor-targeted gene panel, microsatellite instability (MSI) testing, Sanger sequencing for germline MMR gene mutation, immunohistochemistry of MMR proteins, and clinicopathological and survival analysis were performed.

There were many accompanying mutations, suggesting a high tumor mutational burden (TMB) in 84%, but TMB was absent in one case of IDH-wildtype GBM, DMG, medulloblastoma, and PXA, respectively. MLH1, MSH6, MSH2, and PMS2 mutations were found in 44%, 32%, 16% and 12% of patients, respectively. There was one case in which a patient had both MLH1 and PMS2 mutations. MSI-high and MSI-low were found in 41% and 18% of these brain tumors, respectively, and 41% were MSI-stable. All Lynch syndrome-associated GBMs had MSI-high. In addition, 76% (19/25) had histopathologically multinucleated giant cells. Unexpectively, for the cases with O-6-methylguanine methyltransferase (MGMT) methylation and treated with concurrent chemotherapy and radiotherapy with temozolomide, the progression-free survival tended to be better than the patients with no MMRD gliomas, but the number and follow-up duration of our patients were insufficient to get statistical significance.

Through this study, we found the clinicopathological and molecular characteristics of MMRD brain tumor, which have been rarely studied. In particular, characteristics of diffuse midline glioma and anaplastic meningioma with MMRD, and MSH2 p.Tyr405* somatic mutation were new findings that had not been previously reported.

Keywords : mismatch repair gene, Lynch syndrome, microsatellite instability, tumor mutational burden, glioblastoma, familial cancer syndrome

Student Number : 2018-32894

List of Contents

Chapter 1. Introduction 1

1.1. Study Background 1

1.1.1. DNA mismatch repair (MMR) system 1

1.1.2. The relationship between MMR deficiency (MMRD) and Microsatellite Instability (MSI) and tumor mutational burden (TMB) 4

1.1.3. Lynch syndrome 5

1.1.4. MMRD and immunotherapy 6

1.1.5. Previous studies of MMRD brain tumor 7

1.2. Purpose of Research 8

Chapter 2. Body 10

2.1. Materials and methods 10

2.1.1. Case summary 10

2.1.2. Magnetic resonance imaging (MRI) 12

2.1.3. Histopathology and IHC of MMRD brain tumors 12

2.1.4. DNA and RNA extraction for NGS, O-6-methylguanine methyltransferase (MGMT) promoter methylation studies and MSI studies 15

2.1.5. NGS and pipelines of analysis of the somatic mutations 16

2.1.6. Sanger sequencing for germline study 17

2.1.7. R programming **17**

2.1.8. Survival analysis **18**

2.2. Results 28

2.2.1. Imaging, histopathology and IHC 28

2.2.2. Molecular analysis and NGS study 30

2.2.3. Treatment, follow-up of patients, and survival analysis (PFS and OS) 32

2.3. Discussion 42

Chapter 3. Conclusion 51

Acknowledgments 78

Competing interests 78

Ethics approval and consent to participate 78

Bibliography 79

Abstract in Korean 91

List of Figures

Figure 1. The pedigrees of four patients with Lynch syndrome. 19

Figure 2. The brain MRI images of the MMRD brain tumors. 24

Figure 3. The immunohistochemical results of the MMRD brain tumors. 35

Figure 4. The OncoMap of clinicopathological data for 25 MMRD brain tumor cases. 39

Figure 5. The box plot of the number of nonsense mutation of high-grade gliomas with/without MMRD..... 40

Figure 6. The Kaplan-Meier plot of PFS and OS 41

Figure 7. The results of MSI-PCR..... 53

Figure 8. The chromatogram of germline study to know germline MMR gene mutation 54

List of Tables

Table 1. Summary of the clinicopathologic feature of presenting patients with MMRD brain tumors. 2 0

Table 2. The primary antibodies used in this study. 2 6

Table 3. The immunohistochemical and molecular studies include MMR genes, MMR protein and MSI status in our cases. 3 6

Table 4. The list of pathogenic and likely pathogenic mutations found in 25 brain tumors obtained from NGS studies with a comprehensive brain tumor-targeted gene panel..... 5 5

Table 5. The list of the FIRST brain tumor panel established by the Department of Pathology, Seoul National University Hospital (FIRST means Friendly, Integrated, Research-based, Smart and Trustworthy) 7 1

Table 6. Primer sequences used for Sanger germline sequencing. 7 4

Table 7. The list of pathogenic and likely pathogenic mutations found in the initial brain tumors of Case 10, Case 17 and Case 19 through NGS studies with a comprehensive brain tumor-targeted gene panel..... 7 5

Table 8. The comparison of clinicopathological and molecular features of Lynch syndrome-associated MMRD brain tumors and Sporadic MMRD brain tumors 7 7

Abbreviations

MMR : Mismatch repair

MMRD : Mismatch repair deficiency/deficient

HGG : High-grade glioma

IHC : Immunohistochemistry

MLH1 : MutL homolog 1

MSH2 : MutS homolog 2

MSH6 : MutS homolog 6

PMS2 : Postmeiotic segregation increased 2

ADP : Adenosine diphosphate

ATP : Adenosine triphosphate

PCNA : Proliferating cell nuclear antigen

Exo1 : Exonuclease 1

RFC : Replication factor C

MSI : Microsatellite Instability

TMB : Tumor mutational burden

SNP : Single nucleotide polymorphism

MSI-L : Microsatellite Instability-low

MSI-H : Microsatellite Instability-high

MSS : Microsatellite stable

PD-1 : Programmed cell death-1

PD-L1 : Programmed death Ligand 1

ICB : Immune checkpoint blockade

FDA : Food and Drug Administration

NGS : Next-generation sequencing

MGMT : O-6-methylguanine methyltransferase

GBM : Glioblastoma

DMG : Diffuse midline glioma

PXA : Pleomorphic xanthoastrocytoma

CCRT : Concurrent chemotherapy and radiotherapy

TMZ : Temozolomide

MRI : Magnetic resonance imaging

FFPE : Formalin-Fixed Paraffin-Embedded

PCR : Polymerase chain reaction

GK-SRS : Gamma Knife stereotactic radiosurgery

PD : Progressive disease

PR : Partial response

CR : Complete response

GTR : Gross total resection

PO-RT : Post-operative radiotherapy

Chapter 1. Introduction

1.1. Study Background

1.1.1. DNA mismatch repair (MMR) system

Correcting insertion errors of DNA polymerases that occur during DNA replication is a major function of the DNA MMR system [1]. The specificity of MMR is primarily for base-base mismatches and insertion/deletion mismatches generated during DNA replication and recombination [2]. It is the MMR system that is responsible for increasing the replication verity from 100 to 1000 times [3, 4]. The MMR system is involved in S and G2/M phase checkpoints, and is also involved in the apoptosis process to influence DNA damage [5]. MMR is involved in DNA damage signaling in eukaryotic cells, inhibits homologous recombination, and ensures the accuracy and efficiency of somatic hypermutation of the variable regions of immunoglobulin genes, interstrand DNA cross-link repair, repair of aberrant triple-repeat expansions [5].

The DNA MMR system is responsible for the prevention of genomic instability in cells and is controlled by MMR genes [6]. Those are mutL homolog 1 (MLH1), encoded at chromo- some 3p21.3, mutS homolog 2 (MSH2) at chromosome 2p22-21, mutS homolog 6 (MSH6) at chromosome 2p16 and postmeiotic segregation increased 2 (PMS2)

at chromosome 7p22.2 [7].

Proteins called MSH and MLH/PMS, which mediate DNA repair, function as heterodimers [8]. The names of MMR genes reflect their homology with the E. coli system [7]. Thus, MSH was abbreviated from MutS Homolog, and MLH was derived from MutL Homolog of E. coli [7]. The MMR system consists of a group of proteins that interact as heterodimers, which recognize and restore incorrect bases and small loops formed by insertions or deletions [9].

The corrective MSH protein, a product of the gene MSH2, forms a heterodimer with MSH6 and MSH3, correcting mismatched bases. Because MSH6 is expressed 10-fold more than MSH3 [10], heterodimers formed with MSH6 are predominant in human cells. The heterodimers MSH2-MSH6 (also called MutSα) and MSH2-MSH3 (also called MutSβ) bind to mismatches during post-replication DNA strand identification that initiates DNA repair [7]. In the DNA helix, the MSH complex is transformed into a sliding clamp [7]. This sliding clamp slides along the DNA helix until mismatched bases and other extra helix lesions are detected [11]. This mechanism has not yet been fully elucidated and is still under study [12]. MSH2-MSH6 heterodimer recognizes single base mismatches and dinucleotide insertion-removal errors, while MSH2-MSH3 heterodimer detects larger insertion-deletion loops (about 13 nucleotides in length) [13]. After that, when attachment with the MLH1/PMS2 complex occurs, the mutated DNA sequence fragment is degraded and DNA synthesis is restarted [13].

The protein encoded by MSH6 (also known as MutS Homolog 6) is

unstable until it forms a heterodimer with MSH2 to build a mismatch recognition complex [12, 13]. When the MSH2−MSH6 complex recognizes a G/T mismatch, it functions to exchange adenosine diphosphate (ADP) for adenosine triphosphate (ATP) [14]. A highly conserved region exists in the MSH6 gene, which coordinates ATP binding and hydrolysis [14]. After the MSH2−MSH6 heterodimer recognizes and binds to the DNA mismatch, other molecules such as proliferating cell nuclear antigen (PCNA), exonuclease 1 (Exo1), replication factor C (RFC), and MutLα (an MLH1−PMS2 heterodimer) are recruited, then the separation of DNA mismatches occurs [15].

MLH1 can form heterodimers with PMS2, MLH2 (also known as postmeiotic segregation increased 1, PMS1), and MLH3 [7]. The formed heterodimer is recruited to the MMR complex upon the first mismatch detection triggered by either the MSH2−MSH6 heterodimer or the MSH2−MSH3 heterodimer [7]. MutSα bound to DNA mismatches is detected by the MLH1−PMS2 heterodimer and coordinates a series of additional repair steps [16]. In addition, the MLH1−PMS2 complex has endogenous endonuclease activity, so it performs the function of excising unmethylated DNA strands. Single strands excised in this way serve as an entry point for the exonuclease EXO1, which is required for the degradation of mismatched DNA strands, and serve as signaling the initiation of downstream repair processes [12, 17]. The MLH1−PMS2 complex physically interacts with the clamp loader subunit of DNA polymerase delta (Pol δ) and brings the enzyme to the MMR site, thereby

allowing errors that initially deviate from polymerase calibration to be resynthesized by Pol δ [18]. Pol α interacts with the MSH2-MSH6 complex for mismatch repair [19].

PMS2 plays a key role in the nuclear MMR mechanism by forming heterodimers with MLH1 [7]. PMS2 supports genomic integrity by participating in DNA repair as well as DNA damage-induced apoptosis by interacting with p53 and p73 [20]. In addition, PMS2 gene mutations are known to be strongly associated with malignant tumors [21].

The process of the DNA mismatch repair system can be divided into four steps [22, 23]. The first is mismatch recognition by MSH, and the second is MLH recruitment by ATP-bound MSH [22, 23]. The third is cleavage of the DNA strand containing the wrong nucleotide, and the fourth is re-synthesis of the cleavage gap by replicating DNA polymerase using the remaining DNA strand as a template [22, 23].

1.1.2. The relationship between MMR deficiency (MMRD) and Microsatellite Instability (MSI) and tumor mutational burden (TMB)

MMRD can be caused by germline or sporadic mutations or promoter methylation of MMR genes, which is associated with MSI and TMB [24]. Cells with MMRD are mostly characterized by a 102-103 fold increase in spontaneous mutation rates [25, 26]. Increased

mutation rates affect the entire genome, as well as DNA sequences containing microsatellite repeats. [27, 28]. MSI is a change in the length of microsatellite repeats, a type of genomic instability that is prevalent in tumor cells. Consequently, the mutation rate of cells increases with MSI [29]. The presence of MSI-high (MSI-H) [30] is commonly associated with mutations in the MLH1 and MSH2 genes [31, 32]. And MSI-low (MSI-L) is mainly associated with mutations in the MSH6 gene and the PMS2 gene [30]. MSI is a reliable indicator of MMRD in tumors [30, 33].

MMRD contributes to tumorigenesis, poor outcomes, and acquired drug resistance to alkylating agents that mediate the formation of O6 methylguanine-containing mismatches [34, 35]. TMB is considered a potential biomarker for immune checkpoint therapy [36, 37].

1.1.3. Lynch syndrome

Lynch syndrome is an autosomal dominant hereditary cancer syndrome that was originally reported by Warthin in 1913 and is also known as hereditary nonpolyposis colorectal cancer syndrome [38-40]. Lynch syndrome and constitutional MMRD syndrome are caused by heterozygous and homozygous germline mutations in one of the MMR genes, respectively [41, 42]. Germline mutations in MSH2 (40-50%) and MLH1 (30-37%) are the most frequent, and MSH6 and PMS2 mutations are found in 7-13% and up to 9% of cases, respectively [42, 43]. Patients with Lynch syndrome have a lifetime

risk of 50–80% for developing colorectal cancer and 40–60% for developing endometrial cancer and less common cancers of the upper urinary tract, hepatobiliary tract, small intestine, ovary, and skin [44–47]. Lynch syndrome also quadruples the risk of brain tumors, predominantly high-grade gliomas (HGGs) [44–46]. For an accurate diagnosis of sporadic and hereditary MMRD tumors, immunohistochemistry (IHC) of MMR proteins in the tumors, molecular studies to detect MMR gene mutations or methylation, MSI, and genetic testing of affected family members are required [48, 49].

Lynch syndrome-associated MMR deficient (MMRD) tumors often exhibit an MSI-H phenotype [50]. However, since MSI-H is also frequently observed in sporadic colorectal cancers, genetic testing for germline MMR genes is essential [43].

1.1.4. MMRD and immunotherapy

In recent years, immunotherapy has been the focus of improved cancer treatment paradigms resulting in long-lasting tumor remission for both solid and refractory malignancies [51–56]. MMRD, MSI-H, TMB, and programmed death-Ligand 1 (PD-L1) or programmed cell death-1 (PD-1) expression are used as predictive biomarkers to guide the clinical application of immune checkpoint blockade (ICB) therapies [57]. Among many indicators, tumors with MMRD or MSI-H are sensitive to ICB, particularly PD-1 and PD-L1 inhibitors. Thus, for all solid tumors with MMRD and MSI-H, the US

Food and Drug Administration (FDA) approved the ICB indication [58]. Several clinical trials have demonstrated good long-term immunotherapy-related responses and significantly associated better prognosis when colorectal and non-colorectal malignancies with MMRD or MSI-H are treated with immune checkpoint inhibitors [59]. In addition, the anti-PD-1 inhibitor pembrolizumab was approved for refractory or metastatic solid tumor patients with MMRD and MSI-H, and nivolumab was approved for colorectal cancer patients with MMRD and MSI-H [59]. Therefore, recent immunotherapy has improved the therapeutic effect and survival rate of various cancers such as advanced melanoma, non-small cell lung cancer, urothelial cancer, and renal cell cancer [60]. However, it is known that the immunotherapeutic response is not effective in brain tumors with low TMB and is immunologically silent [61-63]. TMB can be increased in MMRD brain tumors, and high TMB responds favorably to checkpoint inhibitors [61]. Previous studies have also shown that GBM with high TMB has a favorable response to anti-PD-1 therapy [64-66]. However, there are very few reports of immunotherapy for MMRD GBM, and further studies are needed [67, 68].

1.1.5. Previous studies of MMRD brain tumor

There have been very few studies of brain tumors with MMRD, and according to a previous study, gliomas with MMRD were rare,

accounting for 1.48% of all gliomas [69]. According to another recent study, 60 germline or somatic MMR gene mutations were identified in 35 cases of primary GBM and 2 cases of recurrent GBM, and the MSH6 and POLE genes were mutated most frequently, and about 60% of mutations were germline mutation [70]. Also, single nucleotide variants were most common, MGMT promoter methylation was observed, and had high TMB [70]. Another previous study researched pediatric malignant brain tumors with constitutional mismatch repair deficiency (CMMRD), including 50 cases of HGG and 6 cases of embryonal tumors [41]. This study reported that histological giant cells, previous malignancies, parental consanguinity, café-au-lait macules, multiple brain tumors, and developmental brain anomalies were the suspect characteristics of CMMRD [41].

1.2. Purpose of Research

Colorectal and endometrial cancers with MMRD have been studied relatively well because of their high frequency [69], but MMRD brain tumors are less well known because of their low frequency.

Therefore, this study aims to study the clinicopathological and molecular features of MMRD brain tumors through 25 patients with MMRD brain tumors associated with sporadic and Lynch syndrome. And we aims to study whether the clinicopathological and molecular genetic characteristics of MMRD brain tumor described by the

previous studies are observed in the cases of this study, and also to study whether new characteristics different from the previous studies are observed. In addition, we aims to make new discoveries by studying the characteristics of MMRD brain tumors of tumor types that have not been studied before, such as diffuse midline glioma and anaplastic meningioma.

Chapter 2. Body

2.1. Materials and methods

2.1.1. Case summary

Among 740 brain tumors from the archives of the Department of Pathology, Seoul National University Hospital, archived from 2017 to 2022 that were subjected to next-generation sequencing (NGS), 25 MMRD brain tumors were found. The tumors included glioblastoma (GBM) IDH-wildtype (n = 17), including one gliosarcoma, astrocytoma IDH-mutant WHO grade 4 (n = 3), diffuse midline glioma (DMG) H3 K27M-mutant (n = 1), anaplastic meningioma (n = 1), oligodendroglioma, IDH-mutant and 1p/19q-codeleted (n = 1), medulloblastoma with extensive nodularity, SHH-activated and TP53-wildtype WHO grade 4 (n = 1) and pleomorphic xanthoastrocytoma (PXA) (n = 1). The proportion of MMRD primary brain tumors in our hospital, including cases of MMRD-associated pineal teratocarcinoma (n = 1) and meningioma (n = 1) that were not included in this study, was ~2.0%. The age of the 25 patients ranged from 1 to 78 years (median age: 47 years), and the male-to-female ratio was 1.5:1.

Fourteen patients had a recurrent brain tumor. Among 14 recurrent brain tumor patients, initial tumor was treated with concurrent

chemotherapy and radiotherapy (CCRT) with temozolomide (TMZ) in 5 patients (4 GBM including 1 gliosarcoma and 1 astrocytoma). And there was one patient (anaplastic meningioma) who was treated with post-operative radiotherapy (PO-RT) for initial tumor, and the remaining 8 patients were those who came to our hospital after receiving treatment for initial tumor from other hospitals. As a result of the IHC and NGS study of the initial tumors, five of them were found to have developed MMRD after CCRT with TMZ. As a result of the NGS study, MMR gene mutation was not observed in the initial tumor in cases 10, 17 and 18 (Tables 4 and 7). And as a result of IHC of MLH1, MSH2, MSH6, and PMS2 in the initial tumor, in cases 1 and 13, no loss was observed, so it could be suggested that there was no MMR gene mutation in the initial tumor of cases 1 and 13.

Four patients had Lynch syndrome, confirmed by the germline Sanger sequencing, but the concurrent malignancy was found in two patients who had histories of extracrainal cancers. The #4 patient had Lynch syndrome with multiple cancers; he was diagnosed with prostatic adenocarcinoma (Gleason score 8) at the age of 61 years and colonic and jejunal cancers at the age of 62 years. His colonic tumors showed a mucinous subtype in the mid-ascending colon and poorly differentiated adenocarcinoma with signet ring cell features in the proximal ascending colon and the jejunum. These subtypes and locations of intestinal adenocarcinoma are known to be associated with Lynch syndrome [71]. Immunohistochemically, the ascending colonic and jejunal adenocarcinomas showed a loss of MSH2 and MSH6 proteins in the tumor cell nuclei, but the MLH1 and PMS2

proteins were retained. Interestingly, prostatic adenocarcinoma is not an MMRD tumor with a retained expression of all four MMR proteins.

The pedigree chart of these four patients with Lynch syndrome suggested an autosomal dominant inheritance of the disease (Figure 1). All patients underwent craniotomy and tumor resection. Clinical manifestations are summarized in Table 1.

2.1.2. Magnetic resonance imaging (MRI)

A total of 84% (21/25) of the tumors were located in the supratentorial area (temporal, frontal, frontotemporal, parietal, or occipital lobes or thalamus or corpus callosum and cingulate gyrus or basal ganglia) (Table 1). Of the remaining four tumors, three tumors are located in the infratentorial area, and one tumor is located in both the supratentorial area and the infratentorial area. MRI revealed high- and low-signal-intensity masses on T2 and T1 imaging, with rim or heterogeneous enhancement and perilesional edema in most patients. All MRI findings suggested high grade brain tumor (Figure 2).

2.1.3. Histopathology and IHC of MMRD brain tumors

Neutral formalin-fixed paraffin-embedded (FFPE) tissues were

cut into slices of 3 μm thickness for H&E staining and IHC. Tissue sections were stained with anti-IDH1 R132H (H09) monoclonal antibody (1:100 dilution, Dianova, Hamburg, Germany), anti-ATRX polyclonal antibody HPA001906 (1:300 dilution, ATLAS ANTIBODIES AB, Bromma, Sweden), anti-p53 monoclonal antibody, DO-7 code M7001 (1:1000 dilution, DAKO, Glostrup, Denmark), anti-pHH3 antibody (1:100 dilution, Cell Marque, Rocklin, USA), anti-Ki67 antibody (1:1000 dilution, DAKO, Glostrup, Denmark), anti- H3K27M (K27M) monoclonal antibody (1:1000 Milipore, Temecula, USA), anti-synaptophysin antibody (1:200 dilution, Novocastra, Newcastle, UK), NeuN (1:500 dilution, Millipore, Temecula, USA), anti-BRAF VE1 antibody (1: 200, Spring Bioscience, CA, US), anti-programmed death 1 NAT105 monoclonal antibody (1:50 Cell Marque, Rocklin, USA), anti-programmed cell death 1 ligand 1 22C3 monoclonal antibody (1:50 DAKO, Glostrup, Denmark), and anti-MMR protein antibodies, including anti-MLH1 M1 monoclonal antibody (1: 50, Ventana, Export, USA), anti-MSH2 G219-1129 monoclonal antibody (1: 200, Ventana, Export, USA), anti-MSH6 44 monoclonal antibody (1: 50, Cell Marque, Rocklin, USA), and anti-PMS2 MRQ-28 monoclonal antibody (1:50, Cell Marque). IHC staining was carried out using a standard avidin-biotin-peroxidase method with a BenchMark ULTRA system (Roche Diagnostics). The primary antibodies used in this study are listed in Table 2.

We used a proper positive control. Most cases had internal positive controls on the slides (Figure 3), and for the negative control, we

omitted the primary antibodies. The Ki67 labeling index was calculated on virtual Leica Biosystems slides (Aperio ScanScope system) using the SpectrumPlus Nuclear Algorithm n9 image analyzer. The positive controls for PD1 and PD-L1 were a known PD1/PD-L1-positive tumor and positive lymphocytes.

Complete loss of expression of MLH1, PMS2, MSH2, or MSH6 in tumor cell nuclei on IHC indicated a loss of the respective protein, and heterogeneous loss of expression was defined as a mixture of areas with loss of expression and retained expression. According to Graham et al.' s paper, heterogeneous MSH6 loss is uncommon but exists and is usually caused by MSI and instability of the MSH6 exon 5 polycytosine tract but is not associated with a germline MSH6 mutation [72].

In the in vivo state, MLH1/PMS2 and MSH2/MSH6 form two functional pairs. When either MLH1 or MSH2 is lost, the partner protein is destabilized and degraded, resulting in the loss of the partner MMR protein. However, the opposite is not true; the absence of PMS2 or MSH6 does not affect stability because MLH1 and MSH2 can bind to and stabilize other molecules [73]. Therefore, we carefully examined the protein expression of these pairs.

Histopathology was reviewed by two pathologists (HK and SHP) according to the histopathological criteria defined by 2021 WHO classification [74] and cIMPACT-NOW updates [75].

2.1.4. DNA and RNA extraction for NGS, O-6-methylguanine methyltransferase (MGMT) promoter methylation studies and MSI studies

Representative areas of the tumor from FFPE tissue on H&E-stained sections with at least 90% tumor cell content were outlined for macrodissection. DNA/RNA extraction was performed from these FFPE tissues using the Maxwell® RSC DNA/RNA FFPE Kit (Promega, USA) according to the manufacturer's instructions. For MSI polymerase chain reaction (PCR) studies using Bethesda's five-marker panel and for the germline MMR mutation study, paired tumor and normal tissue samples were used for genomic DNA extraction. Definitively normal tissue adjacent to the brain tumor was used as the normal counterpart. If it was difficult to find normal tissue on the H&E-stained slide, we verified that it was normal tissue with Ki-67, EGFR, or TP53 immunostaining. If no normal tissue was present in the brain tumor biopsy sample, biopsied extracranial normal tissue or blood was used as the normal counterpart. Genomic DNA was subjected to PCR with fluorescently labeled oligonucleotide primers for five microsatellite loci (BAT25, BAT26, D2S123, D5S346, and D17S250), followed by capillary electrophoresis on an ABI 3100 genetic analyzer (Applied Biosystems, Foster, CA, US). The instability of the investigated loci was defined as a change in the length of the PCR product in a tumor sample compared to the length

of the PCR product in the paired normal sample. MSI status was classified as MSI-H if the sample showed instability at two or more microsatellite loci, MSI-L if the sample showed instability at one locus, and microsatellite stable (MSS) if there was no instability. Methylation-specific PCR was performed using the EZ DNA Methylation Kit (Zymo Research, Irvine, CA) to determine the methylation status of the MGMT promoter.

2.1.5. NGS and pipelines of analysis of the somatic mutations

NGS studies were performed with tumor DNA extracted from FFPE tumor tissue and NEXTSeq Dx505 using a customized brain tumor gene panel (The FIRST brain tumor panel established by the Department of Pathology, SNUH, and approved by the Korea Food and Drug Administration), which assesses 207 brain tumor-associated genes and 54 fusion genes, including 4 MMR genes (Table 5). Fusion genes were sequenced using RNA. Somatic mutations were detected using the Genome Analysis Toolkit (GATK) Mutect2 v4.1.4.1. with default parameters [76]. To avoid germline variant contamination, we used the gnomad.hg19.vcf Genome Aggregation Database (gnomAD) [77] and 1000 g_pon.hg19.vcf files, which include a normal panel for 1000 genomes. The files were provided by the GATK resource bundle. After calling somatic mutations, all variants were annotated by ANNOVAR (https://doc-

openbio.readthedocs.io/projects/ annovar/en/latest/) [78].

We extracted recent 20 cases of IDH-mutant and 60 cases of IDH- wildtype grade 4 gliomas from our hospital NGS data and we compare the number of mutations between MMRD gliomas and non-MMRD gliomas.

2.1.6. Sanger sequencing for germline study

DNA was extracted from FFPE and blood for germline study of MMR genes using a DNA extraction kit (Promega, A2352). Gene-specific primers were added to a 20 μl reaction PCR premix (Bioneer, K-2012). Primers were designed using Primer3 (https://bioinfo.ut.ee/primer3-0.4.0/) (Table 6) [79]. PCR products were analyzed to validate gene mutations using Sanger sequencing.

2.1.7. R programming

Clinical information, mutations, and copy number variations were summarized with Oncoprint data, which were generated using the R package ComplexHeatmap (version 2.7.6.1002, R version 4.0.3) [80]. Progression-free survival (PFS) and overall survival (OS) plots were generated using the R packages Survival (version 3.2-11, R version 4.0.3) and Survminer (version 0.4.9, R version 4.0.3).

2.1.8. Survival analysis

Kaplan-Meier survival analysis was performed, and IDH-wildtype GBMs and DMG with MMRD and IDH-wildtype GBMs with intact MMR were compared. And all case had MGMT methylation and treated with CCRT and TMZ. The control cases consisted of 20 patients who were diagnosed with GBM with MMRD and MGMT methylation and then treated with CCRT and TMZ at the Department of Pathology, Seoul National University Hospital in 2019. PFS was defined as the time from first surgery for the brain tumor to disease progression, while OS was defined as the time from the first surgery for the brain tumor to death.

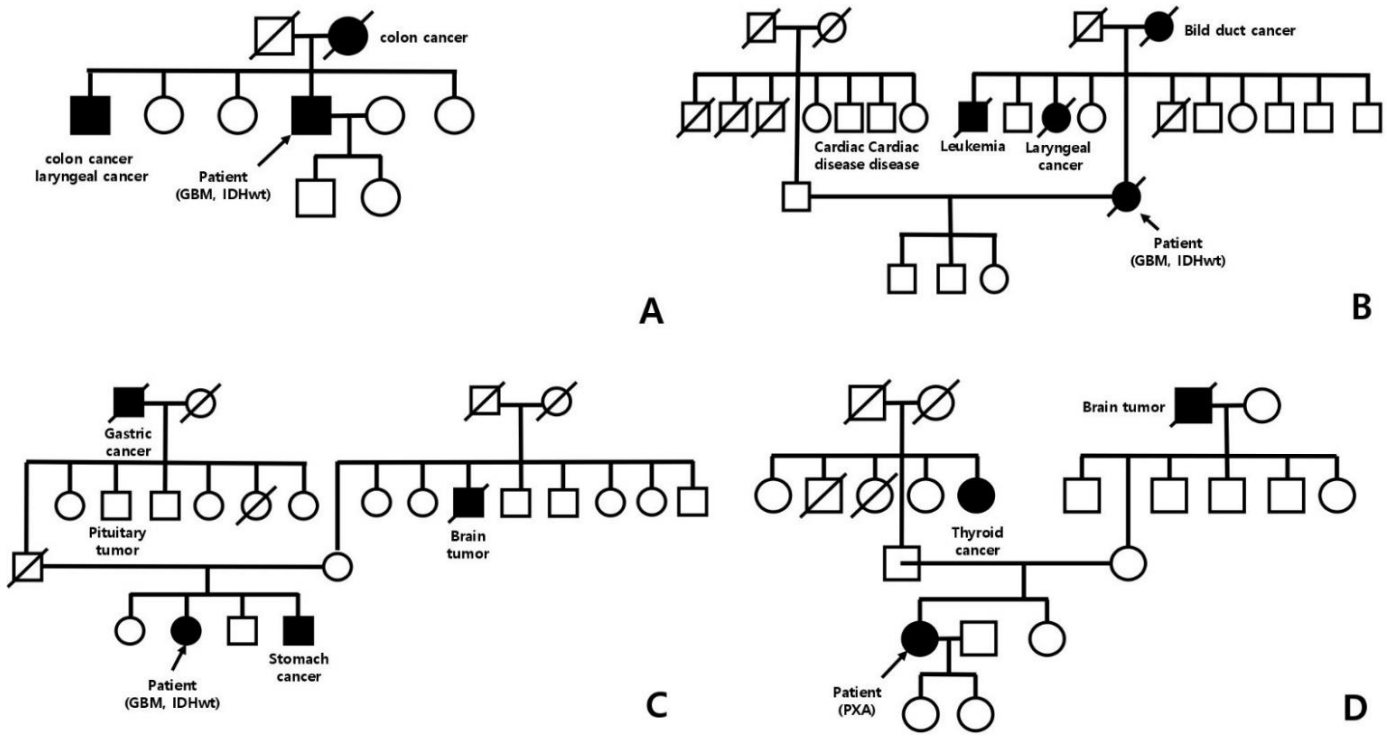

Figure 1. The pedigrees of four patients with Lynch syndrome.

(A) The pedigree of Case 4 shows affected family members with colon cancer or laryngeal cancer. (B) The pedigree of Case 3 shows affected family members with bile duct cancer or laryngeal cancer or leukemia. (C) The pedigree of Case 8 shows affected family members with gastric cancer or brain tumor. (D) The pedigree of Case 25 shows affected family members with thyroid cancer or brain tumor.

Table 1. Summary of the clinicopathologic feature of presenting patients with MMRD brain tumors.

#	Age	Sex	Diagnosis	Accomp-anying tumor	FHx	Site	Tumor size (cm)	MRI finding	Op	Postopera-tive treatment	Follow up	Prese-nce of giant cells	MVP/ Necro-sis	Ki67 index (%)
1	47	F	GBM IDH-wt, rec	MMRD after CCRT/ TMZ	n	Left temporal	5	Rim enhancing mass with hemorrhage	GTR	CCRT/ TMZ, GK-SRS	Recur and died 57 mon after GTR	n (lipidi-zed cells)	p/n	15.70
2	41	F	GBM IDH-wt, rec	none	n	Right parietal	5.7	Heterogeneo-usly enhancing mass	GTR	No adjuvant therapy	Died 12 mon after GTR	p	p/p	79.60
3	75	F	GBM IDH-wt, rec, Lynch syndrome	Colon ADC	p	Right temporal	5	Multifocal enhancing mass	GTR	CCRT/ TMZ	Recur	p	p/p	24.10
4	69	M	GBM IDH-wt, rec, Lynch syndrome	Multiple GI ADC, prostatic cancer	p	Right occipital	6	Heterogeneo-us enhancing mass with perilesional edema	GTR	Hypo-CCRT/ TMZ	Recur	p	p/p	88.80
5	66	M	GBM IDH-wt, rec	none	n	Right frontal	5.3	Irregular enhancing mass	GTR	Hypo-CCRT/ TMZ (Incomple-te)	Recur	p	p/p	37.60

6	73	F	GBM IDH−wt, rec	none	n	Right temporal	1.9	Rim enhancing irregular mass	GTR	PO−RT only	Recur	p	p/p	85.20
7	58	M	GBM IDH−wt	none	n	Posterior fossa*	2.2	Enhancing mass	GTR	CCRT/ TMZ	ST	p	p/n	83.60
8	50	F	GBM IDH−wt, Lynch syndrome	none	p	Left thalamus, basal ganglia, mid−brain	4.6	Enhancing mass lesion	GTR	No adjuvant therapy	ST	p	p/p	63.80
9	31	M	GBM IDH−wt	none	n	Left medial thalamus	2.7	Round mass	GTR	CCRT/ TMZ	Recur (4 mon after Tx)	p	p/p	26.88
10	61	M	GBM IDH−wt, rec	MMRD after CCRT/ TMZ	n	Right frontotemporal	6.5	Rim enhancing cystic mass	GTR	CCRT/ TMZ	Recur (9 mon after Tx)	p	p/p	14.80
11	55	M	GBM IDH−wt, rec	none	n	Left parietal	10.7	Unenhancing mass with perilesional edema	GTR	Palliative hypoRT	ST	p	p/p	80.80
12	46	M	GBM IDH−wt	none	n	Bifrontal, corpus callosum	7.2	Enhancing mass lesion	GTR	CCRT	ST	p	p/p	47.30
13	59	F	GBM IDH−wt, rec	MMRD after CCRT/ TMZ	n	Left parietal	4.1	Heterogeneo−us enhancing mass	GTR	CTx	PR	p	p/p	11.83
14	46	F	GBM IDH−wt	none	n	Right parietotemporal	4.7	Enhancing mass	GTR	CCRT	ST	p	p/p	87.40
15	32	F	GBM IDH−wt	none	n	Right frontal	5.3	Lobulating, necrotic mass	GTR	CCRT/ TMZ	PD	p	p/p	72.60

16	57	M	GBM IDH−wt	none	n	Left frontal	4.5	Enhancing mass with cystic change and perilesional edema	GTR	CCRT/ TMZ	PD	p	p/p	36.60
17	78	M	Gliosarcoma, IDH−wt, rec	MMRD after CCRT/ TMZ	n	Left cerebellum	4	Heterogeneo −us enhancing mass	GTR	CCRT/ TMZ	Recur	p	p/p	18.20
18	11	M	DMG H3 K27M−m, rec	none	n	Right thalamus	3.6	Multiple enhancing solid and cystic mass	GTR	CCRT/ TMZ	Recur (x4) and died 22 mon after GTR	n	p/p	41.80
19	33	M	Astrocytoma, IDH−m, rec	MMRD after CCRT/ TMZ	n	Right frontotemporal	8.5	Enhancing tumor	GTR	No adjuvant therapy	Recur and died 59 mon after GTR	n	p/p	43.10
20	15	M	Astrocytoma, IDH−m, rec	none	n	Right frontal	3.4	Enhancing solid and cystic lesions	GTR	CCRT/ TMZ	Recur	p	p/p	18.80
21	30	M	Astrocytoma, IDH−m	none	p	Right and left frontal, corpus callosum	12	Hyperintense mass with peritumoral edema	GTR	GK−SRS	ST	p	p/p	88.60
22	65	F	Anaplastic meningioma, rec	Breast cancer	n	Right frontal	2.5	Enhancing mass	GTR	RT	ST	n	n/p	23.90
23	39	M	Oligodendro −glioma	none	p	Left frontal	5.6	Large infiltrative	GTR	CCRT	CR	n	p/n	2.60

								T2 high SI lesion						
24	1	M	Medullo-blastoma	none	n	Midline posterior fossa	5	Solid mass	GTR	Follow up loss	Follow up loss	n	n/n	90.40
25	35	F	PXA, Lynch syndrome	none	p	Right frontal, corpus callosum, cingulate gyrus	3.8	Subtle enhancing and cystic change	GTR	No adjuvant therapy	ST	p	n/n	2.20

p, present; n, absent; #, case number; rec, recurrent; GBM IDH-wt, Glioblastoma IDH-wildtype; DMG H3 K27M-m, Diffuse midline glioma H3 K27M-mutant; PXA, Pleomorphic xanthoastrocytoma; ADC, adenocarcinoma; FHx, family history; Posterior fossa*, 4th ventricle and right cerebellum and left vermis; GTR, gross total resection; PO-RT, post-operative radiotherapy; MVP, microvascular proliferation; GK-SRS, Gamma Knife stereotactic radiosurgery; Tx, treatment; CCRT/TMZ, concurrent chemoradiotherapy with temozolomide; PR, partial response; CR, complete response; PD, progressive disease; ST, Stationary; mon, months

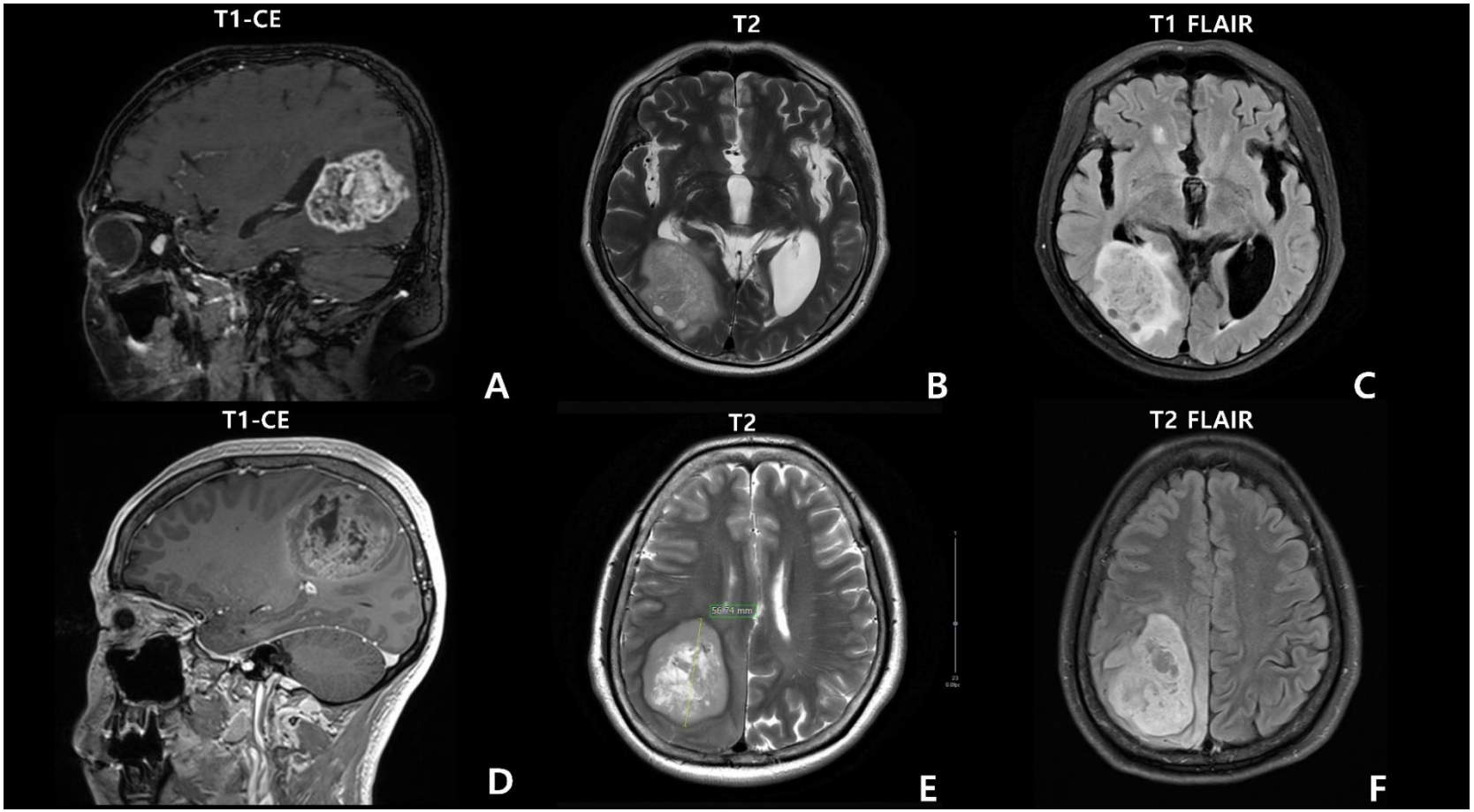

Figure 2. The brain MRI images of the MMRD brain tumors.

(A−C) Case 4 with Lynch syndrome (A) sagittal T1−weighted (postcontrast), (B) axial T2−weighted, and (C) T2 FLAIR MRI results, shows an ~6 cm−long diameters enhancing mass with perilesional edema in the right occipital lobe. (D−F) Case 2 (glioblastoma IDH− wildtype) (D) sagittal T1−weighted (postcontrast), (E) axial T2−weighted, and (F) T2 FLAIR MRI results, revealed a ~5.7 cm heterogeneous mass in the right parietal lobe and midline shift.

Table 2. The primary antibodies used in this study.

Antibody	Dilution	Antigen retrieval	Clone	Source
MLH1	1: 50	Ventana CC1 100°C	M1 (monoclonal)	Ventana, Export, USA
MSH2	1: 200	Ventana CC1 100°C	G219−1129 (monoclonal)	Ventana, Export, USA
MSH6	1: 50	Ventana CC1 100°C	44 (monoclonal)	Cell Marque, Rocklin, USA
PMS2	1: 50	Ventana CC1 100°C	MRQ−28 (monoclonal)	Cell Marque, Rocklin, USA
GFAP	1: 200	Ventana CC1 100°C	6F2 (monoclonal)	DAKO, Glostrup, Denmark
ATRX	1: 200	Ventana CC1 100°C	Polyclonal	Atlas Antibodies AB, Bromma,Sweden
K27M	1: 1000	Ventana CC1 100°C	HH3 (monoclonal)	Milipore, Temecula, USA
Ki67	1: 100	Ventana CC1 100°C	MIB−1 (monoclonal)	DAKO, Glostrup, Denmark
IDH−1	1: 100	Ventaan CC1 100°C	H09 (monoclonal)	Dainova, Hamburg, Germany
P16	1: 100	Ventana CC1 100°C	E6H4 (monoclonal)	Ventana, Export, USA
P53	1: 1000	Ventana CC1 100°C	DO7 (monoclonal)	DAKO, Glostrup, Denmark
pHH3	1: 100	Ventana CC1 100°C	Polyclonal	Cell Marque, Rocklin, USA
Synaptophysin	1: 200	Bond H2O ER2 200°C	27G12 (monoclonal)	NOVO, Newcastle, UK
NeuN	1: 500	Ventana CC1 100°C	A60 (monoclonal)	Millipore, Temecula, USA

BRAF	1:200	Ventana CC1 100°C	VE1 (monoclonal)	Spring Bioscience, CA, US
PD1	1: 50	Ventana CC1 100°C	NAT105 (monoclonal)	Cell Marque, Rocklin, USA
PD-L1(22C3)	1: 50	Ventana CC1 100°C	22C3 (monoclonal)	DAKO, Glostrup, Denmark

MLH1, MutL Protein Homolog 1; MSH2, Mut-S-homologue-2; MSH6, Mut-S-homologue-6; PMS2, post-meiotic segregation increased 2; GFAP, glial fibrillary acidic protein; ATRX, Alpha Thalassemia associated mental retardation X; K27M, Histon lysin27methionine; IDH-1, isocitrate dehydrogenase 1; pHH3, phosphorylated Histone H3; PD-1, programmed death 1; PD-L1, programmed cell death 1 ligand 1

2.2. Results

2.2.1. Imaging, histopathology and IHC

The locations of the MMRD brain tumors were the temporal (n = 3), parietal (n = 3), occipital (n = 1), frontal (n = 6) lobes, thalamus (n = 2), frontotemporal lobe (n = 2), bifrontal lobes and corpus callosum (n = 1), parietotemporal lobe (n =1), right and left frontal lobe and corpus callosum (n = 1), midline posterior fossa (n = 1), right frontal lobe and corpus callosum and cingulate gyrus (n = 1), 4th ventricle and right cerebellum and left vermis (n = 1), Left thalamus and basal ganglia and midbrain (n = 1), cerebellum (n = 1) (Table 1). On MRI of high grade brain tumors, the tumors showed high and low signal intensity on T2 and T1 imaging, respectively, with rim or heterogeneously enhanced parts (Figure 2) of variable sizes, ranging from 1.9 to 12 cm.

Histopathologically, 19 tumors (76%) showed marked bizarre multinucleated giant cells (Table 1, Figure 3A, E). The remaining three tumors did have somewhat pleomorphic nuclei but did not have numerous multinucleated giant cells (Table 1, Figure 3I). Microvascular proliferation was observed in 22 cases (88%), and necrosis was observed in 20 cases (80%).

Among the ten MLH1−mutant tumors, complete loss of both MLH1 and PMS2 IHC in the tumor cells was present in three cases (cases #1, 17, and 18) (Figure 3J, 3K), and three cases showed

heterogeneous loss of MLH1 and no loss of the partner protein PMS2 (case #9, 13, and 16) and two cases showed heterogeneous loss of MLH1 and PMS2 (case #15 and 24) and one case showed complete loss of MLH1 and heterogeneous loss of PMS2 (case #19) and one case showed complete loss of MLH1 and no loss of PMS2 (case #12).

Among the eight MSH6-mutant tumors, complete loss of MSH6 and no loss of the partner protein MSH2 IHC in the tumor cells was present in five cases (case #3, 8, 11, 20, and 25) (Figure 3B, 3C, 3N, 3O), and two cases showed heterogeneous loss of MSH6 and no loss of MSH2 (case #10 and 21) and one case showed heterogeneous loss of MSH6 and MSH2 (case #23).

Four MSH2-mutant tumors showed complete loss of MSH2 IHC but a heterogeneous loss of the partner protein MSH6 (Patient #2, 4, 5, and 6) (Figure 3F, 3G) (Table 3).

Two (Cases #7 and 22) PMS2-mutant tumors had complete loss of PMS2 only.

One case with mutations in both MLH1 and PMS2 showed heterogeneous loss of both MLH1 and PMS2 IHC in the tumor cells.

These results were expected because it is already known that MLH1 and MSH2 loss can result in a heterogeneous loss of the partner protein PMS2 and MSH6 because MLH1/PMS2 and MSH2/MSH6 form two functional pairs, but MSH6-mutant tumors are known to have no partner protein loss [72].

PD-L1 was weakly positive in 1% of tumor cells in three cases (cases #6, 8, and 17), focally positive in about 30% of tumor cells in two cases (cases # 10 and 11), and a few positive in 4/HPF tumor

cells in one case (case # 15) but it was not expressed in the other cases. PD-1 was positive in a few immune cells in cases #6, 8, and 10 (positive in up to 4 cells/HPF) and was not expressed in the other tumors. The Ki-67 labeling index ranged from 2.2% to 90.4% (Table 1). IHC results of our study are summarized in Table 3.

2.2.2. Molecular analysis and NGS study

MSI-H was found in 41% (9/22) of patients (Figure 7) including three Lynch syndrome-associated cases (case #3, #4 and #8), MSI-L was found in four patients (18%), and nine patients (41%) exhibited MSS. The MSI study could not be performed in the remaining three cases because there was no normal tissue (Table 3). MGMTp methylation was found in 52.2% (12/23) of tumors, and among GBMs (including gliosarcoma), 47.1% (8/17) of them had MGMTp methylation.

The NGS studies found MMR gene mutations as well as multiple pathogenic mutations and variants of uncertain significance (Figure 4). The variants of MLH1 were p.Ser685Phe/c.2054C>T, p.His264Asn/c.790C>A,p.Arg226*/c.676C>T,p.Ser252Leu/c.755C>T,p.Ser95Ala/c.283T>G,p.Arg127Ile/c.380G>T,p.Ala353fs/c.1057delG,p.Arg687Trp/c.2059C>T,p.Arg385Cys/c.1153C>T,and p.Arg265Cys/c.793C>T.

The variants of MSH2 were p. Leu372*/c.1115T>A, p.Tyr405*/c.1215C>A, p.Gln510*/c.1528C>T, and splicing/c.1511-

1G>A. The variants of MSH6 were p.Ser602*/c.1805C>G, p.Arg1172fs/c.3514dupA,p.Arg1334Gln/c.4001G>A,p.Gln889fs/c.2665dupC,p.Phe1088fs/c.3261dupC,p.Gln958*/c.2872C>T,p.Trp97*/c.291G>A,p.Arg1035*/c.3103C>T,p.Cys1062Tyr/c.3185G>A,p.Gly1157Asp/c.3470G>A,p.Thr1219Ile/c.3656C>T,p.Arg1242Cys/c.3724C>T, and p.Ala36Val/c.107C>T. The variants of PMS2 were p.Thr337fs/c.1009dupA,p.Arg315*/c.943C>T,p.Arg107Trp/c.319C>T and p.Val321Ala/c.962T>C. The MMR gene mutations were verified by IHC (Figure 3). Notably, the MSH2 p.Tyr405* mutation found in patients with Lynch syndrome is a known germline variant but has never been reported as a somatic mutation in the OnkoKB and Cosmic databases [81].

TP53 showed the highest frequency of pathogenic variants, with variants found in 18 cases (p.Arg273His/c.818G>A, p.Arg273Cys/c.817 C>T,p.Arg175His/c.524G>A, p.Arg248Gly/c.742C>G,p.Arg342*/c.1024C>T,p.Arg248Trp/c.742C>T,p.Val173Leu/c.517G>T,p.Arg213Gln/c.638G>A,p.Gly245Ser/c.733G>A,p.Arg213*/c.637C>T,p.Arg267Trp/c.799C>T,p.Arg248Gln/c.743G>A, .Arg282Leu/c.845G>T,p.Lys382fs/c.1146delA,p.Gly244Cys/c.730G>T,p.Arg282Trp/c.844C>T,p.Arg65*/c.193A>T,p.His179Arg/c.536A>G).

Other frequent pathogenic variants were CDKN2A/2B hemizygous deletion and mutations (p. Ala36fs/c.106delG, p.His83Tyr/c.247 C>T, p.Thr79Ile/c.236C>T) found in 12 tumors, and NF1 mutations (single or both alleles; p.Ser82Phe/c.245 C>T, p.Trp426*/c.1278 G>A, p.Trp1559*/c.4677G>A,splicing/c.6642+1G>A,p.Asn78fs/c.233dupA,p.Arg2258*/c.6772C>T,splicing/c.1185+1G>T,p.Pro1421Gln/c.42

62C>A,p.Ile679fs/c.2033dupC,p.Arg1611Gln/c.4832G>A,p.Arg1611Trp/c.4831C>T, p.Trp2369*/c.7107 G>A, and p.Arg1769*/c.5305C>T,p.Cys1960fs/c.5878delT,p.Cys1960fs/c.5878delT,p.Arg1204Leu/c.3611G>T,p.Gln2303*/c.6907C>T,p.Leu1880*/c.5639T>A,p.Ser82Phe/c.245C>T) and NF1 deletion were found in 10 tumors (Table 4).

The number of nonsense mutation was higher in MMRD-HGG (average 23.0-23.6) than HGGs without MMRD (average 4.7-5.8) (Figure 5). Of the 4 MMRD brain tumors with low mutation numbers (less than 5 single nucleotide polymorphism (SNP)), GBM IDH-wt (Case #7) had many copy number aberrations, but the remaining DMG (Case #18), medulloblastoma (Case #24) and PXA (Case #25) did not have many copy number aberrations, eventhough they had MMRD (Table 4).

Germline studies of MMR genes by Sanger sequencing revealed germline mutations in three cases (Cases #3, #8, and #25, Figure 8). In one remaining patient, the germline study could not be performed because there was no normal tissue or blood. This patient had multiple organ tumor history and additional clinicopathological reviews suggested Lynch syndrome-associated MMRD brain tumor.

2.2.3. Treatment, follow-up of patients, and survival analysis (PFS and OS)

After the surgery, ten patients with GBM, DMG, and astrocytoma

were treated with CCRT with TMZ, and two patients with GBM were treated with Hypo-CCRT and TMZ. Three patients with GBM, and Oligodendroglioma were treated with CCRT and one patient with GBM was treated with chemotherapy only. Three patients with GBM and Anaplastic meningioma were received radiotherapy only and one patient with astrocytoma underwent Gamma Knife stereotactic radiosurgery (GK-SRS). However, four of the five remaining patients did not receive adjuvant therapy and follow-up for the other patient was lost. (Table 1). The intestinal carcinoma of a Lynch syndrome patient (Case # 4) who had been treated with post-operative adjuvant 5-fluorouracil, leucovorin, and oxaliplatin did not recur for 8 years. Instead, this patient' s MMR-intact prostatic adenocarcinoma metastasized to multiple bones, including the rib, thoracic spine, sacrum, and pelvic bones, during the last 7 years, despite radiation therapy, chemotherapy (docetaxel and abiraterone/prednisone), and androgen deprivation therapy.

Eleven patients (44%) had recurrences of tumors. Two other GBM patients who received CCRT with TMZ had progressive disease (PD), and the other GBM patient who received chemotherapy only had a partial response (PR). One patient with oligodendroglioma who received CCRT achieved a complete response (CR). The eight remaining patients remained stationary status. Four patients (16%) died from diseases. Case #1 recurred after 1 year of treatment, despite gross total resection (GTR) of the tumor plus CCRT and GK-SRS, and died 57 months after the initial surgery. Case #2 died at 12 months after GTR with no adjuvant therapy, and case #18 died at 22

after GTR and CCRT with recurrences. Case #19 with astrocytoma IDH-mutant recurred in 39 months and died in 59 months after GTR. PFS of the patients with recurrent tumors was 1 month to 42 months.

Kaplan-Meier survival analysis was performed on nine patients diagnosed with IDH wildtype GBM and DMG with MMRD and MGMT methylation and then treated with CCRT and TMZ. The control group consisted of 20 patients who were diagnosed with GBM without MMRD and with MGMT methylation and then treated with CCRT and TMZ at the Department of Pathology, Seoul National University Hospital in 2019.

Kaplan-Meier survival analysis showed a trend for lower PFS in GBM patients without MMRD than those in HGG (GBM and DMG) patients with MMRD ($p = 0.17$) (Fig. 6A). There was no difference in OS between GBM patients without MMRD and HGG patients with MMRD ($p=1$) (Fig. 6B). However, the results did not have a statistical significance due to the small number of cases, short follow-up duration, and also better patient care. ($P>0.05$).

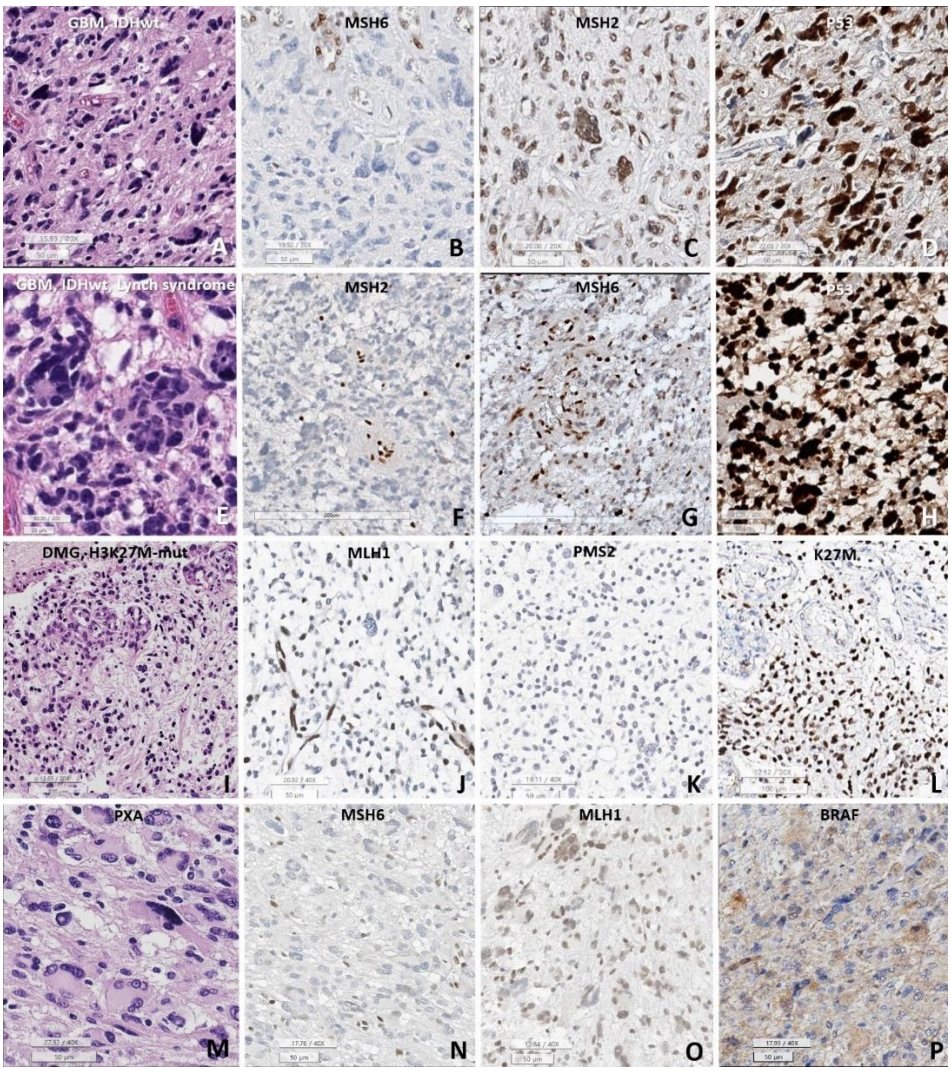

Figure 3. The immunohistochemical results of the MMRD brain tumors.

(A–D) GBM IDH−wt with Lynch syndrome and MSH6 mutation (Case 3), (E–H) GBM IDH−wt with Lynch syndrome and MSH2 mutation (Case 4), (I–L) DMG H3 K27M−m (Case 18) and (M−P) PXA with MSH6 mutation (Case 25). (A, E) Bizarre multinucleated giant cells (Cases 3 and 4) were predominant. (B, C) MSH6−mutant tumors showed loss of MSH6 expression but no loss of MSH2 (F, G) MSH2−mutant case (Case 4) showed loss of MSH2 but heterogeneous loss of MSH6(D, H) P53 staining showed overexpression in both Case 3 and Case 4. (I) The DMG H3 K27M−mutant showed no bizarre multinucleated giant cells but did show microvascular proliferation. (J, K) MLH1 and PMS2 loss were present. (L) K27M staining showed nuclear positivity. (M) PXA with Lynch syndrome case showed marked multinucleated giant cells and vacuolar cells and stroma. (N) There was loss of MSH6 expression, but (O) the expression of MLH1 was retained. (P) BRAF VE1 staining was positive. (A, E, I, M: H&E; C, F: MSH2; B, G, N: MSH6; D, H: P53; J, O: MLH1; K: PMS2; L: K27M; P: BRAF. Bar size: A–D, H, J, K, M–P: 50 micrometers; E: 20 micrometers; F, G: 200 micrometers; I, L: 100 micrometers).

Table 3. The immunohistochemical and molecular studies include MMR genes, MMR protein and MSI status in our cases.

#	Diagnosis	Mutant MMR gene, variant allele frequency	MLH1/PMS2	MSH2/MSH6	MSI	7p+ &10q−/EGFR amplification/PTEN loss	BRAF mut	TERT promoter mut	ATRX/IDH1/K27M	PD1/PDL1	MGMT methyl−ation
1	GBM IDH−wt, rec	MLH1, p.Ser685Phe, 36.09%, likely pathogenic	Loss/Loss	No loss/No loss	MSS	n/n/p	n	p	p/n/n	n/n	p
2	GBM IDH−wt, rec	MSH2, p.Leu372*, 94.66%, pathogenic	No loss/No loss	Loss/Loss*	MSI−H	n/n/p	n	n	p/n/n	n/n	n
3	GBM IDH−wt, rec, Lynch syndrome	MSH6, p.Ser602*, 48.62%, pathogenic	No loss/No loss	No loss/Loss	MSI−H	n/n/n	n	n	p/n/n	n/n	n
4	GBM IDH−wt, rec, Lynch syndrome	MSH2, p.Tyr405*, 92.89%, pathogenic	No loss/No loss	Loss/Loss*	MSI−H	n/n/n	n	n	p/n/n	n/n	p
5	GBM IDH−wt, rec	MSH2, p.Gln510*, 16.26%, pathogenic	No loss/No loss	Loss/Loss*	MSI−L	n/n/p	n	p	p/n/n	n/n	p
6	GBM IDH−wt, rec	MSH2, splicing, 14.55%, pathogenic	No loss/No loss	Loss/Loss*	MSS	n/n/n	n	p	p/n/n	a few (+) /weak (+)	p
7	GBM IDH−wt	PMS2, p.Thr337fs, 57.02%, pathogenic	No loss/Loss	No loss/No loss	MSS	n/n/n	n	n	p/n/n	n/n	n
8	GBM IDH−wt, Lynch syndrome	MSH6, p.Phe1088fs, 23.86%/ p.Gln889fs, 44.46%, pathogenic	No loss/No Loss	No loss/Loss	MSH−H	n/n/n	n	n	p/n/n	a few (+) /weak (+)	n

9	GBM IDH−wt	MLH1, p.His264Asn, 3.06%, pathogenic	Loss*/No loss	No loss/No loss	ND	n/n/p	n	n	p/n/n	n/n	n
10	GBM IDH−wt, rec	MSH6, p.Gln958*, 21.1%, pathogenic	No loss/No loss	No loss/ Loss*	MSS	n/n/n	n	p	p/n/n	a few (+) /focal (+)	p
11	GBM IDH−wt, rec	MSH6, p.Trp97*, 9.11%/p.Arg1035*, 5.84%/ p.Cys1062Tyr, 7.22%/p.Gly1157Asp, 7.03%, pathogenic	No loss/ No loss	No loss/Loss	MSI −H	n/p/p	n	p	p/n/n	n /focal (+)	p
12	GBM IDH−wt	MLH1, p.Arg226*, 89.15%	Loss/No loss	No loss/ No loss	MSI −H	n/n/n	n	n	p/n/n	n/n	n
13	GBM IDH−wt, rec	MLH1, p.Ser252Leu, 45.13%	Loss*/No loss	No loss/ No loss	MSH −L	n/p/n	n	n	p/n/n	n/n	p
14	GBM IDH−wt	MLH1, p.Arg265Cys, 40.57%, pathogenic PMS2, p.Arg315*, 38.31%/ p.Arg107Trp, 34.78%, pathogenic	Loss*/Loss*	No loss/No loss	MSI −H	n/n/n	n	n	p/n/n	n/n	n
15	GBM IDH−wt	MLH1, p.His264Asn, 5.87%, pathogenic	Loss*/Loss*	No loss/No loss	MSS	n/n/n	n	n	p/n/n	n /a few (+)	n
16	GBM IDH−wt	MLH1, p.Ser95Ala, 53.45%, pathogenic	Loss*/No loss	No loss/No loss	MSH −L	n/n/p	n	p	p/n/n	n/n	n
17	Gliosarcoma, IDH−wt, rec	MLH1, p.Arg127Ile, 5.4%, pathogenic	Loss/Loss	No loss/No loss	MSS	n/n/n	n	n	p/n/n	n /weak (+)	p

18	DMG H3 K27M−m, rec	MLH1, p.Ala353fs, 54.29%, likely pathogenic	Loss/Loss	No loss/No loss	MSI−H	n/n/p	n	n	n/n/p	n/n	n
19	Astrocytoma, IDH−m, rec	MLH1, p.Arg687Trp, 87.09%, pathogenic	Loss/Loss*	No loss/No loss	MSI−H	n/n/n	n	n	n/p/n	n/n	p
20	Astrocytoma, IDH−m, rec	MSH6, p.Arg1172fs, 80.49%, pathogenic	No loss/ No loss	No loss/Loss	ND	n/n/n	n	n	p/p/n	n/n	n
21	Astrocytoma, IDH−m	MSH6, p.Thr1219Ile, 5.08%/ p.Arg1242Cys, 4.58%, pathogenic	No loss/No loss	No loss/ Loss*	MSS	n/n/n	n	n	n/p/n	n/n	p
22	Anaplastic meningioma, rec	PMS2, p.Val321Ala, 14.33%, pathogenic	No loss/Loss	No loss/No loss	MSH−L	n/n/n	n	n	N/D	n/n	N/D
23	Oligodendroglioma	MSH6, p.Ala36Val, 44.56%, pathogenic	No loss/No loss	Loss*/Loss*	MSS	n/n/n	n	p	p/p/n	n/n	p
24	Medulloblastoma	MLH1, p.Arg385Cys, 47.58%, pathogenic	Loss*/Loss*	No loss/ Loss*	ND	n/n/n	n	n	N/D	n/n	N/D
25	PXA, Lynch syndrome	MSH6, p.Arg1334Gln, 55.06%, pathogenic	No loss/No loss	No loss/Loss	MSS	n/n/n	p	n	p/n/n	n/n	p

#, case number; p, positive or present; n, negative or absent; Loss*, Heterogeneous loss of expression; MSS, microsatellite stable; MSI−H, microsatellite instability−high; MSI−L, microsatellite instability−low; weak (+), weakly positive (+/3) in 1% of tumor cells; A few (+), positive in up to 4/HPF; focal (+), positive up to 30%; 7p+&10q−, the concurrent gain of whole chromosome 7 and loss of whole chromosome 10; ND, not done; mut, mutation

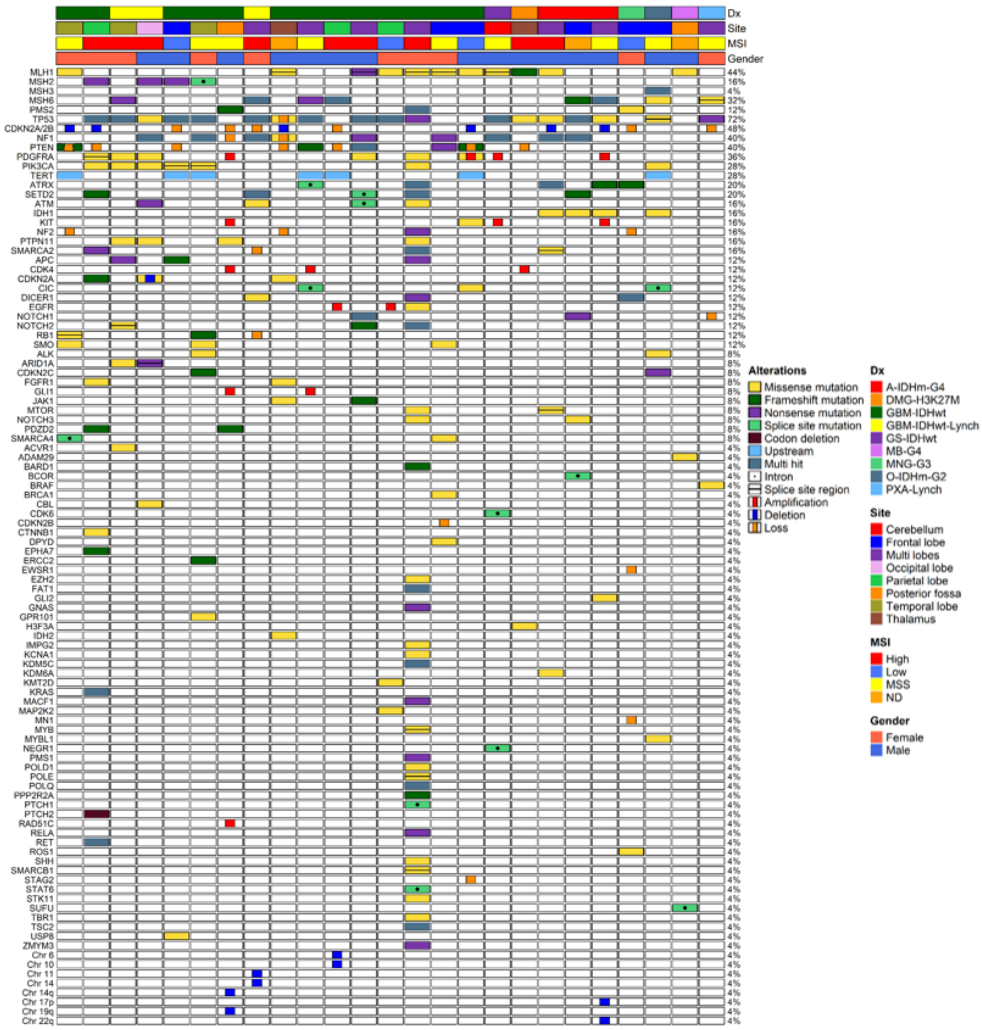

Figure 4. The OncoMap of clinicopathological data for 25 MMRD brain tumor cases.

Clinicopathological and molecular genetic features and NGS results of 25 cases listed in the OncoMap System. GS, gliosarcoma; A-IDHm-G4, Astrocytoma, IDH-m, WHO grade 4; MB-G4, Medulloblastoma, WHO grade 4; MNG-G3, Anaplastic meningioma, WHO grade 3; O-IDHm-G2, Oligodendroglioma, IDH-mutant, WHO grade 2; Dx, diagnosis

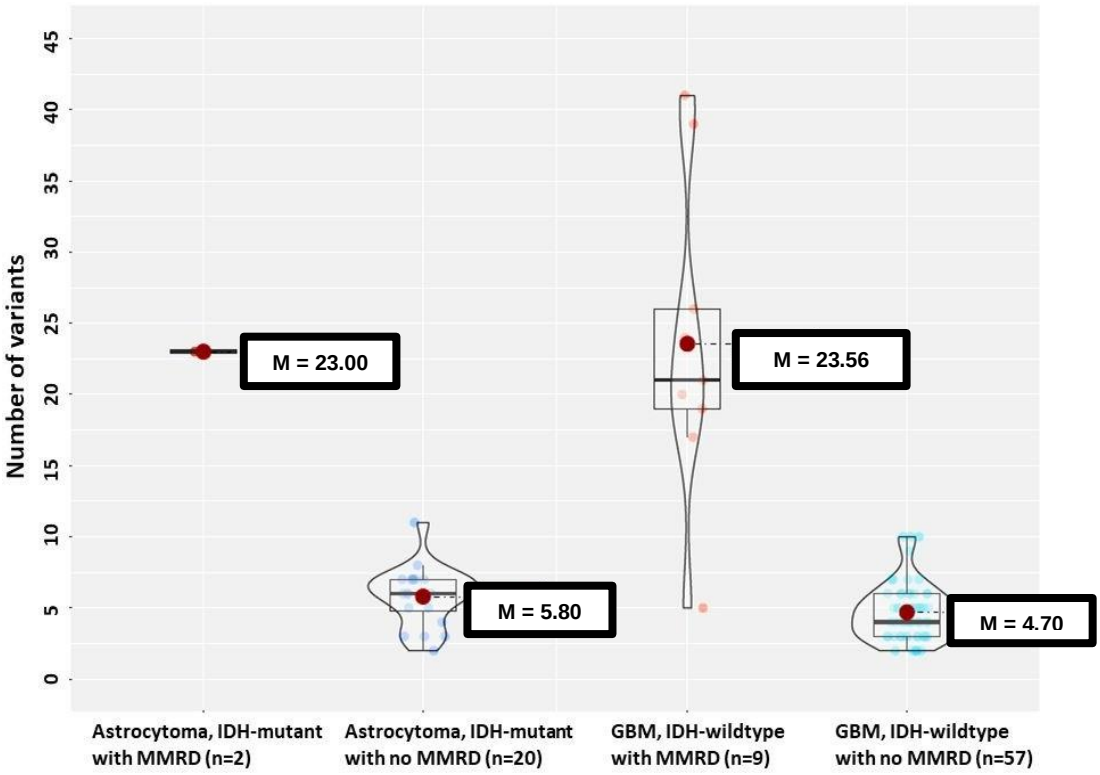

Figure 5. The box plot of the number of nonsense mutation of high-grade gliomas with/without MMRD.

MMRD high-grade gliomas had higher number of nonsense mutation than non-MMRD gliomas; The average number of mutations in astrocytoma IDH-mutant with MMRD and without MMRD is 23.0 and 5.8, respectively. The average number of mutations in glioblastoma, IDH-wildtype with MMRD and without MMRD was 23.6 and 4.7, respectively.

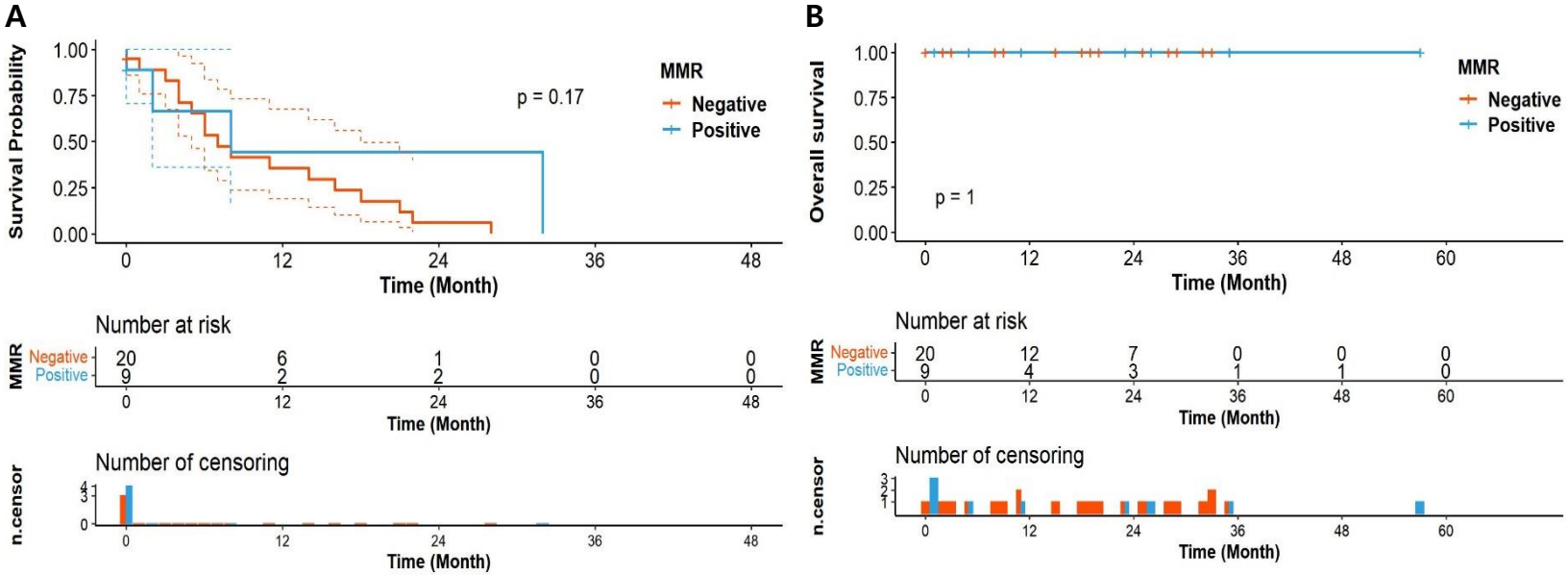

Figure 6. The Kaplan-Meier plot of PFS and OS

The Kaplan-Meier plot of PFS (A) and OS (B) for IDH-wildtype GBM and DMG with MMRD and IDH-wildtype GBM without MMRD. (A : p = 0.17, B : p = 1)

2.3. Discussion

MMRD brain tumors are very rare, accounting for ~2% of primary brain tumors, and are also histopathologically diverse, including GBM, astrocytoma, oligodendroglioma, gliosarcoma, anaplastic PXA, medulloblastoma, and neuroblastoma [82]. Among them, GBM and high-grade astrocytoma are the most common sporadic or inherited MMRD brain tumors [44, 83]. The proportion of MMRD primary brain tumors in the 740 brain tumors studied with NGS in our hospital for 3 years was ~2%, which include 4 Lynch syndrome-related and 5 CCRT-induced MMRD brain tumors.

In line with our results, the inactivation of MMR genes has been identified in both IDH-mutant and IDH-wildtype gliomas [84]. Pediatric high-grade gliomas, such as DMG H3 K27M-altered, medulloblstoma, and anaplastic PXA also have MMRD [85] and deficiency of MMR genes also has been identified in anaplastic meningioma and oligodendroglioma. Lynch syndrome is the most common form of hereditary colorectal cancer, accounting for 2-7% of all cases of colorectal cancer [86]. Extracolonic tumors of Lynch syndrome include cancers of the small bowel, pancreas, urinary tract, prostate, and brain [44, 86]. The presence of monoallelic germline MMR gene defects is essential for the diagnosis of Lynch syndrome. Constitutional MMRD syndrome has biallelic germline mutations in MMR genes, is autosomal recessive, and usually has severe nuclear pleomorphism and multinucleated giant cells, as is seen in Lynch

syndrome-associated gliomas [41, 83]. Our Lynch syndrome patients had a germline MSH2 mutation (p.Tyr405*/c.1215C>A) and MSH6 mutation (p.Ser602*/c1805C>G,p.Arg1334Gln/c.4001G>A, p.Phe1088fs/c.3261dupC, p.Gln889fs/c.2665dupC), which have previously been reported in a Lynch syndrome patient [81, 87]. However, POLE and MUTYH gene mutations can also be diagnostic for Lynch syndrome [86].

Comparing the clinicopathological and molecular genetic characteristics of Lynch syndrome-associated MMRD brain tumors and Sporadic MMRD brain tumors observed in this study, Lynch syndrome-associated MMRD brain tumors have a lower median age and occur more in women than men. And all tumors occurred in the supratentorial area, histologically, giant cell features were observed in all cases. And MSI-H was observed more in Lynch syndrome-associated MMRD brain tumors (75%) than in Sporadic MMRD brain tumors (33%) (Table 8).

We obtained MMRD-associated genes from cBioportal, namely, CHEK1, CHEK2, RAD51, BRACA1, BRACA2, MLH1, MSH2, ATM, ATR, MDC1, PARP1, and FANCF. Among them, MSH2 defects were found in 0.2% of the GBMs and 0.6% of all primary brain tumors in TCGA data. To explore MMRD-associated primary brain tumors, we downloaded the gene profiles of primary brain tumors from cBioportal (TCGA database) (oncoprint.svg). The MSH2 mutation-associated MMRD brain tumors included 43 gliomas, including GBM (n=20), oligodendroglioma (n=9), anaplastic oligodendroglioma (n=6), diffuse astrocytoma (n=5), anaplastic astrocytoma (n=2), and

oligoastrocytoma (n=1). Missense mutation was the most common type of mutation in MMR genes, found in 65.1% (28/43) of cases, and nonsense and splice mutations were found in 21% and 12% of cases, respectively. There was one case each with frameshift and insertion mutations. In our study, frameshift mutation was observed in MLH1 gene(p.Ala353fs/c.1057delG),MSH6 gene(p. Phe1088fs/c.3261dupC, p.Gln889fs/c.2665dupC, p.Arg1172fs/c.3514dupA), and PMS2 gene (p.Thr337fs/c.1009dupA). And splicing mutation was observed in MSH2 gene (splicing/c.1511-1G>A).

GBMs are usually chromosomally unstable, thus commonly have chromosomal aberrations and aneuploid DNA content [88]. Unlike the conventional GBM IDH-wildtype [75, 89], our 17 cases of MMRD GBM IDH-wildtype did not have the concurrent gain of chromosome 7 and loss of chromosome 10. And in only 2 of 17 cases, amplification of the EGFR gene was observed. Instead, MMRD gliomas had mutations in TP53, NF1, and PIK3CA, amplification of PDGFRA, and deletion of CDKN2A/2B. Variable PTEN alteration, including frame shift mutation (n=3) and loss (n=6) was found in 53% (9/17). TERT promoter (TERTp) mutation (C250T and C228T) was present in 35% (6/17) (Table 3, Figure 4). In our study, there were 9 cases with MSS despite MMRD but all our Lynch syndrome associated HGG had MSI-H.

Gliosarcoma IDH-wildtype usually have TP53 and PTEN mutations and CDKN2A deletions, but EGFR amplification is rare [90]. In this study, the gliosarcoma IDH-wildtype had two TP53 mutations (p.Arg248Trp, c.742C>T and p.Val173Leu, c.517G>T) and

NF1 mutation (splicing, c.1185+1G>T and p.Pro1421Gln, c.4262C>A), and PDGFRA amplification; however, neither PTEN mutation nor CDKN2A deletion was present. DMG H3 K27M-mutant can have TP53 mutation (approximately 50% of cases) and ATRX mutation (loss of expression; 10–15% of cases) [91]. Our MMRD DMG H3 K27M-mutant also had TP53 mutation (p.Arg273His, c.818G>A, VAF 43%) and no ATRX mutation. Astrocytoma IDH-mutant WHO grade 4 can have CDKN2A/B homozygous deletion [92], and this gene deletion was found in two out of three astrocytoma IDH-mutant in this study. The molecular features of anaplastic meningioma are NF2 mutations or Loss of 6q, 9p, 10q, 14q or Gains of 1q, 9q, 15q, 17q, 20q or Deletion of 1p21 or CDKN2A Deletion or TERT promoter mutations [93]. In this study, anaplastic meningioma with MMRD, there was a copy number loss in the NF2 gene and CDKN2A deletion was observed. Our PXA case had BRAF mutation (p.Val600Glu, c.1799T>A). IDH-mutation and 1p/19q-codeletion were observed in oligodendroglioma, and medulloblastoma was genetically SHH-activated and TP53-wildtype, so MMRD oligodendroglioma and medulloblastoma did not show any special molecular features different from the existing molecular characteristics.

Inactivating mutations of TP53 and chromosomal instability following the loss of MMR function are common genetic abnormalities [88]. However, because colorectal carcinomas usually have diploid or near-diploid DNA content with a few chromosomal aberrations, colorectal carcinomas with MMRD usually do not have inactivating

mutations of TP53 and chromosomal instability [88]. The MMRD IDH-wildtype and IDH-mutant HGGs in this study commonly had additional pathogenic missense mutations of the TP53, NF1, PIK3CA, deletion or mutation of CDKN2A/2B, amplification or mutation of PDGFRA. In addition, copy number aberrations of various genes and many other VUS, suggesting a high TMB.

Because of the presence of mutations in the TP53, NF1, and ATM genes, concomitant or underlying Li-Fraumeni, neurofibromatosis type 1, or ataxia-telangiectasia cancer syndrome needed to be ruled out. However, these cancer-predisposing syndromes require germline mutations for diagnosis, and the associated tumor types are different from those seen in our Lynch syndrome cases; Li-Fraumeni syndrome-associated cancers are usually sarcomas, breast cancers, brain tumors, and leukemias [94]. Brain tumors of Li-Fraumeni syndrome can appear as low-grade gliomas or HGGs [95]. Patients with neurofibromatosis type 1 typically have neurofibroma, optic nerve glioma, or neurofibrosarcoma, and patients with ataxiatelangiectasia syndrome usually have non-Hodgkin lymphoma and leukemia [94].

TMZ is an alkylating agent that induces methylation at the guanine O6 position in DNA [96]. And the methylated O6-guanine aberrantly pairs with thymine, a mechanism by which the mismatch repair system cleaves the DNA double helix and induces apoptosis of cancer cells [96]. There was a study on cases where MMRD occurred in tumors that recurred after TMZ treatment [97, 98]. In this study, 5 cases developed MMRD in tumors that recurred after TMZ treatment.

It is thought that a mutation associated with TMZ occurred within a key amino acid of the MMR gene, resulting in MMRD [96].

Hypermutation can occur in recurrent tumors after TMZ treatment via MMRD and MSI-H- related mechanisms, whereas these alterations are extremely rare in primary brain tumors [99]. MMRD is often associated with MSI, and it is one of the mechanisms behind acquired resistance to the alkylating chemotherapeutic agent TMZ in gliomas [99].

MMRD is also related to TMB and neoantigen loads, therefore, can be a target of immunotherapy. Generally, MMRD tumors have MSI-H [50]. MSI-H is generally uncommon in sporadic brain tumors, but if it is present, it may represent MMR gene germline mutation carriers [100]. Although one study reported that MSI is rare in Lynch syndrome-associated brain tumors [101], it can occur as a result of the loss of MMR function [50]. Our 3 Lynch associated HGG had MSI-H. The TMB could not be verified in our cases due to the limitations of the targeted gene panel (207 brain tumor-targeted genes and 54 fusion genes), but most of our cases possibly had TMB because of many pathogenic and likely pathogenic mutations and VUS. However, four cases (1 GBM IDHwt, 1 PXA, 1 DMG, 1 medulloblastoma) had less than 5 SNPs with variable copy number aberrations (Figure 4, Table 4).

Among MMRD-associated tumors, the number of methylated genes is known to be the lowest in brain tumors and the highest in colorectal cancers [102]. Methylation of MGMT promoter was observed in about half (52.2%) of our MMRD cases. The methylation

of MGMT promoter is known to occur in approximately half of MMR-intact gliomas; therefore, the incidence of MGMT promoter methylation in MMRD gliomas could be similar to that in MMR-intact gliomas [103].

MGMT reduces the effectiveness of TMZ by removing the methyl group at the O-6 position of guanine [104]. Therefore, silencing the promoter of MGMT via DNA hypermethylation sensitizes GBM tumors to TMZ [104]. Studies have shown that GBM with MGMT promoter methylation is correlated with improved survival when treated with TMZ [105]. And although it was not a significant result, even in this study, when GBM with MGMT metylation was treated with TMZ, the OS was not poor.

According to a recent study, replication repair-deficient (RRD) HGGs have a global methylation pattern distinct from that of replication repair-intact HGGs [106]. This methylation pattern varies according to key driver mutations (for example, the IDH1 R132H and H3F3A K27M mutations) and the location of the tumor. Even in the same RRD HGG case, the methylation patterns of the initial tumor and recurrent tumor can be different. In addition to the methylation pattern, hypomethylation in specific gene pathways associated with critical cellular functions occurs in RRD HGG, which can be used as a target for treatment. Therefore, methylation patterns should be studied to help classify and treat MMRD gliomas.

Loss of nuclear MMR protein was 100% correlated with MMR gene mutation in our cases, suggesting that IHC is sufficient to identify MMRD in brain tumors. MLH1/PMS2 and MSH2/MSH6 form two

functional pairs in vivo. Loss of MLH1 or MSH2 destabilizes and degrades the partner protein, so MLH1/PMS2 and MSH2/MSH6 pair losses are common [107]. However, the opposite is not true; the absence of PMS2 or MSH6 does not affect the stability of the partner protein, because MLH1 and MSH2 can bind to and stabilize other molecules [73]. Therefore, the expression of these protein pairs must be carefully investigated. Most of our cases showed these patterns.

MMRD is often associated with MSI-H and TMB, which can contribute to poor outcomes [34, 35]. Unexpectedly, Kaplan-Meier survival analysis showed a trend for lower PFS in IDH-wildtype GBM patients without MMRD than in IDH-wildtype GBM and DMG patients with MMRD ($p = 0.17$), when having MGMT methylation and treated with CCRT and TMZ. In other analyses, PFS and OS were not significantly different between glioma patients with and without MMRD ($P > 0.05$) (Figure 6), possibly due to the limited number of MMRD cases and the short follow-up duration. To determine the biological behavior of MMRD brain tumors, more large-scale, well-designed prospective studies are required. Randomized controlled trials are necessary to improve the treatment of MMRD patients.

PD1/PD-L1 IHC staining was almost negative in our cases. Identifying patients with MMRD brain tumors is important for appropriate treatment strategies for patients with sporadic MMRD tumors and family members at risk for Lynch syndrome or CMMRD. Since the PD1/PD-L1 IHC staining was negative in most of our MMRD brain tumors, other options, such as direct identification of

MMRD via NGS or IHC studies in primary brain tumors, may be needed to determine the indications for immunotherapy. These MMRD gliomas could be sensitive to immunotherapy but resistant to TMZ [108].

Chapter 3. Conclusion

We analyzed 21 sporadic MMRD and 4 Lynch syndrome-associated primary brain tumors in this study, representing a rare event population, about 2.0% of the primary brain tumor cases in our hospital. Most (88%) cases were grade 4 except for anaplastic meningioma, which was WHO grade 3, and PXA and oligodendroglioma, which were WHO grade 2. MMRD developed after CCRT in 5 cases, which were both IDH-mutant and wildtype gliomas. These MMRD gliomas contained many pathogenic and benign or likely benign mutations and VUS, suggesting high TMB, but one GBM, DMG, medulloblastoma, and PXA did not have TMB despite the MMRD. 41% of our MMRD-brain tumors and all Lynch syndrome-associated GBMs had MSI-H. Genetic profile of MMRD-associated GBMs was different from that of conventional GBMs. The MMRD GBM did not have EGFR amplification, PTEN homozygous deletion, or concurrent 7p gain and 10q loss. TERT promoter mutation was found in only 35% (6/17) of IDH-wildtype MMRD GBMs. MGMT promoter methylation was found in 52% of our cases. The PFS of our MMRD patient had a tendency of lately recurrence but OS did not identify the worse prognosis of patients with MMRD brain tumors than controls with MMR-intact brain tumors, possibly due to the small number of cases and the short follow-up period in half of the cases. Through this study, we found the clinicopathological and molecular characteristics of MMRD brain tumor, which have been rarely studied. In particular,

characteristics of diffuse midline glioma and anaplastic meningioma with MMRD, and MSH2 p.Tyr405* somatic mutation were new findings that had not been previously reported. MMRD gliomas with TMB and MSI-H are sensitive to immunotherapy and resistant to TMZ. If the clinical pathologic and molecular genetic characteristics of MMRD brain tumor found through this study are helpful in the diagnosis of MMRD brain tumor, it will help predict the therapeutic potential through immunotherapy and help in the selection of appropriate treatment. More studies are needed in the form of clinical trials of immunotherapy for MMRD brain tumors.

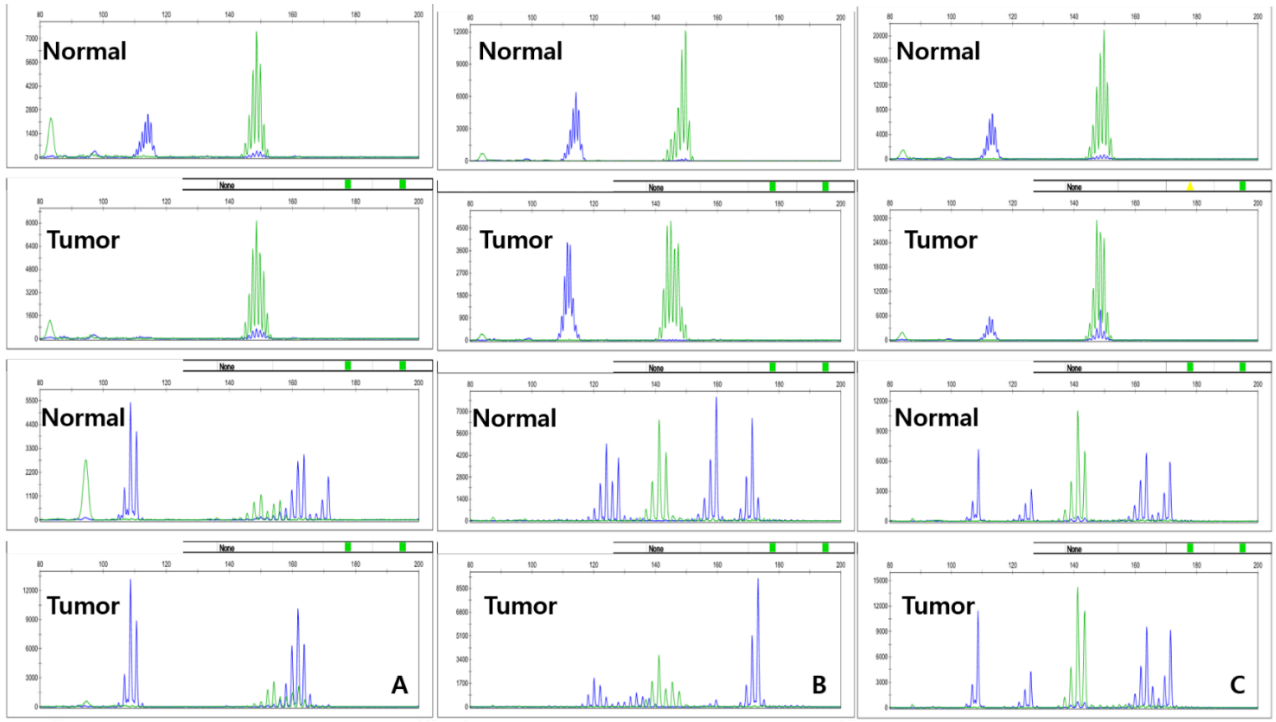

Figure 7. The results of MSI-PCR

MSI-H was found in (A) GBM IDH-wildtype (patient 2), (B) GBM IDH-wildtype with Lynch syndrome (patient 4), and (C) another GBM IDH-wildtype (patient 3).

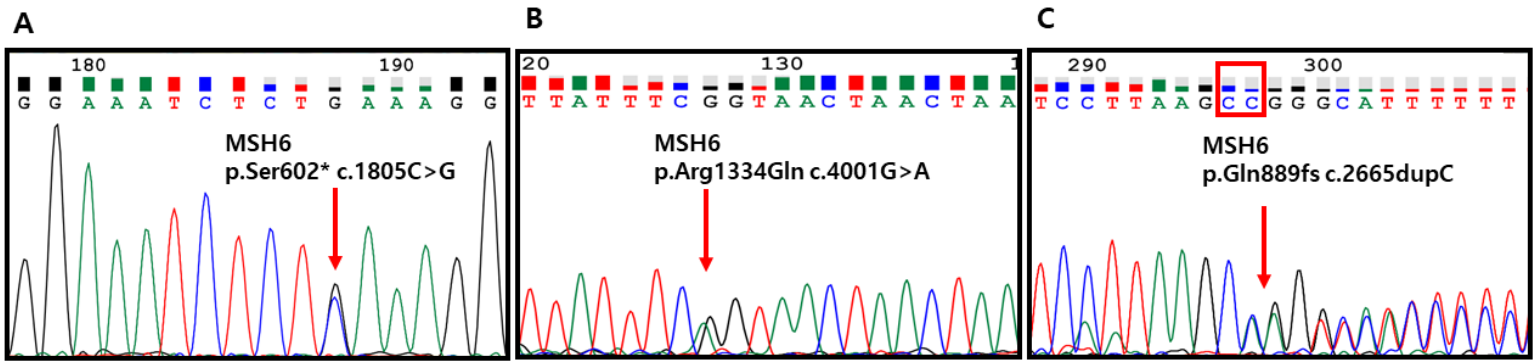

Figure 8. The chromatogram of germline study to know germline MMR gene mutation

It showed (A) MSH6 gene missense mutation (p.Ser602*/c.1805C>G) in patient 3, (B) MSH6 gene missense mutation (p.Arg1334Gln/c.4001G>A) in patient 25, (C) MSH6 gene frameshift mutation (p.Gln889fs/c.2665dupC) in patient 8.

Table 4. The list of pathogenic and likely pathogenic mutations found in 25 brain tumors obtained from NGS studies with a comprehensive brain tumor−targeted gene panel.

#	C	Pos	Ref	Alt	Gene	Ref seq	E	Effect	AA	CDS	Pathogenic	Read	Alt	Ref	Vaf %
1	13	49027129	G	A	RB1	NM_000321.2	18	Non_synonymous_coding+splice_site_region	p.Asp566Asn	c.1696G>A	Likely Pathogenic	1757	319	1438	18.16
	7	1.29E+08	C	T	SMO	NM_005631.4	4	Non_synonymous_coding	p.Leu267Phe	c.799C>T	Likely Pathogenic	4832	375	4457	7.76
	10	89720856	AC	A	PTEN	NM_001304717.2	9	Frame_shift	p.Ser511fs	c.1527delC	Likely Pathogenic	2133	792	1341	37.13
	9				CDKN2A/2B			Homozygous deletion							
	3	37090459	C	T	MLH1	NM_000249.3	18	Non_synonymous_coding	p.Ser685Phe	c.2054C>T	Likely Pathogenic	3433	1239	2194	36.09
	22				NF2			Loss							
	19	11121208	G	A	SMARCA4	NM_001128849.1	15	Splice_site_donor+intron	splicing	c.2274+1G>A	Pathogenic	1874	453	1421	24.17
	5	1295250	G	A	TERT	NM_198253.2		Upstream	C250T	c.−146C>T	Pathogenic	117	47	70	40.17
	10				PTEN			Loss							
2	9				CDKN2A/2B			Hemizygous deletion							
	10				PTEN			Loss							
	1	45293688	CAGA	C	PTCH2	NM_003738.4	14	codon_deletion	p.Ser628del	c.1882_1884delTCT	Pathogenic	258	129−129	353	42.23
	2	47656919	T	A	MSH2	NM_000251.2	7	stop_gained	p.Leu372*	c.1115T>A	Pathogenic	780	445−335	44	94.66
	3	41266074	A	G	CTNNB1	NM_001904.3	3	non_synonymous_coding	p.His24Arg	c.71A>G	Pathogenic	790	404−386	1157	40.58
	3	47162413	GA	G	SETD2	NM_014159.6	3	frame_shift	p.Ser1238fs	c.3712delT	Pathogenic	866	433−433	1235	41.22
	3	178916876	G	A	PIK3CA	NM_006218.2	2	non_synonymous_coding	p.Arg88Gln	c.263G>A	Pathogenic	504	241−263	740	40.51
	4	55161294	C	T	PDGFRA	NM_006206.4	23	non_synonymous_coding+splice_site_region	p.Ser1042Leu	c.3125C>T	Pathogenic	523	280−243	845	38.23

	5	32091103	A	AC	PDZD2	NM_178140.2	19	frame_shift	p.Arg2519fs	c.7554dupC	Pathogenic	325	162–163	478	40.47
	6	93956640	G	GA	EPHA7	NM_004440.3	15	frame_shift	p.His866fs	c.2595dupT	Pathogenic	512	256–256	1067	32.43
	8	38277149	C	T	FGFR1	NM_001174067.1	10	non_synonymous_coding	p.Val427Ile	c.1279G>A	Pathogenic	998	499–499	331	75.09
	9	2039690	C	T	SMARCA2	NM_001289396.1	4	stop_gained	p.Arg194*	c.580C>T	Pathogenic	172	83–89	46	78.9
	9	21974720	GC	G	CDKN2A	NM_000077.4	1	frame_shift	p.Ala36fs	c.106delG	Pathogenic	234	117–117	73	76.22
	10	43601863	G	A	RET	NM_020975.4	5	non_synonymous_coding	p.Val303Met	c.907G>A	Pathogenic	141	78–63	212	39.94
	10	43601863	G	A	RET	NM_020975.4	5	non_synonymous_coding	p.Val303Met	c.907G>A	Pathogenic	141	78–63	212	39.94
	12	25368389	AT	A	KRAS	NM_033360.3	5	frame_shift	p.Lys185fs	c.555delA	Pathogenic	157	78–79	160	49.53
	12	25368421	T	TC	KRAS	NM_033360.3	5	frame_shift	p.Glu175fs	c.523dupG	Pathogenic	218	109–109	243	47.29
	17	7577121	G	A	TP53	NM_000546.5	8	non_synonymous_coding	p.Arg273Cys	c.817C>T	Pathogenic	684	306–378	898	43.24
	17	7578406	C	T	TP53	NM_000546.5	5	non_synonymous_coding	p.Arg175His	c.524G>A	Pathogenic	282	147–135	337	45.56
3	2	1.59E+08	C	T	ACVR1	NM_001111067.2	9	non_synonymous_coding	p.Ala383Thr	c.1147G>A	Likely pathogenic	1779	147	1632	8.26
	1	1.21E+08	C	T	NOTCH2	NM_024408.3	4	non_synonymous_coding +splice_site_region	p.Gly139Asp	c.416G>A	Likely pathogenic	1279	543	736	42.46
	5	1.12E+08	C	T	APC	NM_000038.5	16	stop_gained	p.Arg2237*	c.6709C>T	Pathogenic	2075	93	1982	4.48
	1	27099873	G	A	ARID1A	NM_006015.4	15	non_synonymous_coding	p.Gly1251Asp	c.3752G>A	Pathogenic	1515	466	1049	30.76
	2	48026927	C	G	MSH6	NM_000179.2	4	stop_gained	p.Ser602*	c.1805C>G	Pathogenic	1701	827	874	48.62
	3	1.79E+08	A	G	PIK3CA	NM_006218.2	21	non_synonymous_coding	p.His1047Arg	c.3140A>G	Pathogenic	1589	256	1333	16.11
	12	1.13E+08	C	T	PTPN11	NM_002834.3	3	non_synonymous_coding	p.Ala72Val	c.215C>T	Pathogenic	2223	686	1537	30.86
	17	7578211	C	T	TP53	NM_000546.5	6	non_synonymous_coding	p.Arg213Gln	c.638G>A	Pathogenic	1566	443	1123	28.29
	17	7578406	C	T	TP53	NM_000546.5	5	non_synonymous_coding	p.Arg175His	c.524G>A	Pathogenic	943	423	520	44.86
4	11	1.08E+08	C	T	ATM	NM_000051.3	50	stop_gained	p.Arg2486*	c.7456C>T	Pathogenic	661	251	410	37.97

	11	1.19E+08	T	C	CBL	NM_005188.3	9	non_synonymous_coding	p.Cys419Arg	c.1255T>C	Likely pathogenic	1055	424	631	40.19
	2	47657019	C	A	MSH2	NM_000251.2	7	stop_gained	p.Tyr405*	c.1215C>A	Pathogenic	253	235	18	92.89
	4	55152105	A	T	PDGFRA	NM_006206.4	18	non_synonymous_coding	p.Asp846Val	c.2537A>T	Likely pathogenic	1050	151	899	14.38
	1	27100207	C	T	ARID1A	NM_006015.4	16	stop_gained+splice_site_region	p.Arg1335*	c.4003C>T	Pathogenic	1148	470	678	40.94
	12	1.13E+08	C	T	PTPN11	NM_002834.3	3	non_synonymous_coding	p.Ala72Val	c.215C>T	Pathogenic/likely pathogenic	1197	69	1128	5.76
	9	21971111	G	A	CDKN2A	NM_000077.4	2	non_synonymous_coding	p.His83Tyr	c.247C>T	Likely pathogenic	1064	935	129	87.88
	9				CDKN2A			Hemizygous deletion							
	17	29553477	A	AC	NF1	NM_001042492.2	18	frame_shift	p.Ile679fs	c.2033dupC	Pathogenic	669	30	639	4.48
	17	29592354	G	A	NF1	NM_001042492.2	36	non_synonymous_coding	p.Arg1611Gln	c.4832G>A	Likely pathogenic	312	119	193	38.14
	17	29670071	G	A	NF1	NM_001042492.2	48	stop_gained	p.Trp2369*	c.7107G>A	Pathogenic	597	79	518	13.23
	3	1.79E+08	T	C	PIK3CA	NM_006218.2	12	non_synonymous_coding	p.Cys604Arg	c.1810T>C	Likely pathogenic	510	202	308	39.61
	17	7577120	C	T	TP53	NM_000546.5	8	non_synonymous_coding	p.Arg273His	c.818G>A	Pathogenic	707	661	46	93.49
5	2	47693814	C	T	MSH2	NM_000251.2	10	stop_gained	p.Gln510*	c.1528C>T	Pathogenic	246	40	206	16.26
	3	178917478	G	A	PIK3CA	NM_006218.2	3	non_synonymous_coding+splice_site_region	p.Gly118Asp	c.353G>A	Pathogenic	70	21	49	30
	5	1295228	G	A	TERT	NM_198253.2		upstream	C228T	c.−124C>T	Pathogenic	77	21	56	27.27
	5	112174873	A	AT	APC	NM_000038.5	16	frame_shift	p.Ser1196fs	c.3586dupT	Pathogenic	348	38	310	10.92
	15	50784990	T	C	USP8	NM_001128610.2	15	non_synonymous_coding	p.Leu776Pro	c.2327T>C	Pathogenic	840	60	780	7.14
	17	7577121	G	A	TP53	NM_000546.5	8	non_synonymous_coding	p.Arg273Cys	c.817C>T	Pathogenic	1378	100	1278	7.26
	17	7579470	CG	C	TP53	NM_000546.5	4	frame_shift	p.Val73fs	c.216delC	Pathogenic	2009	62	1947	3.09
	9				CDKN2A			Loss							

	9				CDKN2B			Loss							
	10				PTEN			Loss							
6	1	51436140	C	CA	CDKN2C	NM_078626.2	1	frame_shift	p.Asn35fs	c.104dupA	Pathogenic	762	134	628	17.59
	2	29449800	C	T	ALK	NM_004304.4	18	non_synonymous_coding	p.Val1019Ile	c.3055G>A	Pathogenic	1510	243	12667	16.09
	2	47693796	G	A	MSH2	NM_000251.2	9	splice_site_acceptor+intron	splicing	c.1511−1G>A	Pathogenic	275	40	235	14.55
	3	178917478	G	A	PIK3CA	NM_006218.2	3	non_synonymous_coding+splice_site_region	p.Gly118Asp	c.353G>A	Pathogenic	177	34	143	19.21
	5	1295250	G	A	TERT	NM_198253.2		upstream	C250T	c.−146C>T	Pathogenic	138	41	97	29.71
	7	128845583	G	A	SMO	NM_005631.4	4	non_synonymous_coding	p.Val294Ile	c.880G>A	Pathogenic	1638	272	1366	16.61
	13	48881488	C	CAG	RB1	NM_000321.2	2	frame_shift	p.Ala74fs	c.219_220dupAG	Pathogenic	213	33	180	15.49
	17	7577120	C	T	TP53	NM_000546.5	8	non_synonymous_coding	p.Arg273His	c.818G>A	Pathogenic	1235	28	1207	2.27
	17	7577548	C	T	TP53	NM_000546.5	7	non_synonymous_coding	p.Gly245Ser	c.733G>A	Pathogenic	2290	752	1538	32.84
	17	29486049	GA	G	NF1	NM_001042492.2	3	frame_shift	p.Asn78fs	c.233delA	Pathogenic	221	41	180	18.55
	17	29557360	AG	A	NF1	NM_001042492.2	23	frame_shift	p.Arg1026fs	c.3075delG	Pathogenic	492	65	427	13.21
	19	45856056	G	GC	ERCC2	NM_000400.3	20	frame_shift	p.Ala617fs	c.1849dupG	Pathogenic	838	161	677	19.21
	X	136113491	C	T	GPR101	NM_054021.1	1	non_synonymous_coding	p.Ala115Thr	c.343G>A	Pathogenic	1619	290	1329	17.91
7	5	31799656	A	AG	PDZD2	NM_178140.2	1	frame_shift	p.Lys104fs	c.308dupG	Pathogenic	587	84	503	14.31
	7	6029565	G	GT	PMS2	NM_000535.5	10	frame_shift	p.Thr337fs	c.1009dupA	Pathogenic	114	65	49	57.02
	12	112888199	C	T	PTPN11	NM_002834.3	3	non_synonymous_coding	p.Ala72Val	c.215C>T	Pathogenic	1577	377	1200	23.91
	4				PDGFRA			Amplification							
	4				KIT			Amplification							

	9				CDKN2A			Loss							
	9				CDKN2B			Loss							
	12				GLI1			Amplification							
	12				CDK4			Amplification							
	17				NF1			Loss							
	17				RAD51C			Amplification							
	14							14q deletion							
	19							19q deletion							
8	2	48027786	G	GC	MSH6	NM_000179.2	4	frame_shift	p.Gln889fs	c.2665dupC	Pathogenic	713	317	396	44.46
	2	48030639	A	AC	MSH6	NM_000179.2	5	frame_shift	p.Phe1088fs	c.3261dupC	Pathogenic	721	172	549	23.86
	3	47147534	G	A	SETD2	NM_014159.6	6	stop_gained	p.Arg1598*	c.4792C>T	Pathogenic	943	377	566	39.98
	3	47155365	C	T	SETD2	NM_014159.6	5	splice_site_donor+intron	splicing	c.4715+1G>A	Pathogenic	499	194	305	38.88
	11	108199839	C	T	ATM	NM_000051.3	49	non_synonymous_coding	p.Ser2394Leu	c.7181C>T	Pathogenic	108	70	38	64.81
	14	95560469	A	G	DICER1	NM_030621.4	26	non_synonymous_coding	p.Leu1707Pro	c.5120T>C	Pathogenic	726	40	686	5.51
	17	7577139	G	A	TP53	NM_000546.5	8	non_synonymous_coding	p.Arg267Trp	c.799C>T	Pathogenic	1268	498	770	39.27
	17	7577538	C	T	TP53	NM_000546.5	7	non_synonymous_coding	p.Arg248Gln	c.743G>A	Pathogenic	2486	1012	1474	40.71
	17	29592353	C	T	NF1	NM_001042492.2	36	non_synonymous_coding	p.Arg1611Trp	c.4831C>T	Pathogenic	398	142	256	35.68
	17	29654553	C	T	NF1	NM_001042492.2	38	stop_gained	p.Arg1769*	c.5305C>T	Pathogenic	641	233	408	36.35
	17	29661916	GT	G	NF1	NM_001042492.2	40	frame_shift	p.Cys1960fs	c.5878delT	Pathogenic	448	180	268	40.18
	11							deletion							
	14							deletion							

	9				SMARCA2			Loss							
	9				CDKN2A			Loss							
	9				CDKN2B			Loss							
	13				RB1			Loss							
9	1	65312368	C	T	JAK1	NM_002227.2	14	Non_synonymous_coding	p.Val651Met	c.1951G>A	Pathogenic	1594	749	845	46.99
	3	37056035	C	A	MLH1	NM_000249.3	9	Non_synonymous_coding +s plice_site_region	p.His264Asn	c.790C>A	Pathogenic	1733	53	1680	3.06
	8	38274849	G	T	FGFR1	NM_001174067.1	13	Non_synonymous_coding	p.Asn577Lys	c.1731C>A	Pathogenic	1202	897	305	74.63
	9	21971122	G	A	CDKN2A	NM_001195132.1	2	Non_synonymous_coding	p.Thr79Ile	c.236C>T	Pathogenic	117	53	64	45.30
	15	90628598	A	C	IDH2	NM_002168.3	8	Non_synonymous_coding	p.Met330Arg	c.989T>G	Pathogenic	1328	580	748	43.67
	17	7577093	C	A	TP53	NM_001126112.2	8	Non_synonymous_coding	p.Arg282Leu	c.845G>T	Pathogenic	1021	35	986	3.43
	17	29560134	G	T	NF1	NM_001042492.2	27	Non_synonymous_coding	p.Arg1204Leu	c.3611G>T	Pathogenic	1164	37	1127	3.18
	9				CDKN2A			Deletion							
	9				CDKN2B			Deletion							
	10				PTEN			Loss							
	17				TP53			Loss							
	17				NF1			Loss							
	22				NF2			Loss							
10	2	48027994	C	T	MSH6	NM_000179.2	4	stop_gained	p.Gln958*	c.2872C>T	Pathogenic	711	150	561	21.10
	5	1295228	G	A	TERT	NM_198253.2		non_synonymous_coding	C228T	c.−124C>T	Pathogenic	135	24	111	17.78
	10	89720785	CAAGG	C	PTEN	NM_000314.6	8	frame_shift	p.Lys313fs	c.939_942delGGAA	Pathogenic	140	41	99	29.29

	17	7578212	G	A	TP53	NM_000546.5	6	stop_gained	p.Arg213*	c.637C>T	Pathogenic	1625	361	1264	22.22
	17	7578437	G	A	TP53	NM_000546.5	5	stop_gained	p.Gln165*	c.493C>T	Pathogenic	3304	1140	2164	34.50
	19	42798975	G	A	CIC	NM_015125.4	19	splice_site_acceptor+intron	splicing	c.4460−1G>A	Pathogenic	1403	147	1256	10.48
	X	76888873	C	T	ATRX	NM_000489.4	18	splice_site_acceptor+intron	splicing	c.4957−1G>A	Pathogenic	517	99	418	19.15
	12				GLI1			Amplification							
	12				CDK4			Amplification							
11	2	48018096	G	A	MSH6	NM_000179.2	2	stop_gained	p.Trp97*	c.291G>A	Pathogenic	538	49	489	9.11
	2	48028225	C	T	MSH6	NM_000179.2	4	stop_gained	p.Arg1035*	c.3103C>T	Pathogenic	411	24	387	5.84
	2	48030571	G	A	MSH6	NM_000179.2	5	non_synonymous_coding	p.Cys1062Tyr	c.3185G>A	Pathogenic	374	27	347	7.22
	2	48032080	G	A	MSH6	NM_000179.2	6	non_synonymous_coding	p.Gly1157Asp	c.3470G>A	Pathogenic	782	55	727	7.03
	5	1295228	G	A	TERT	NM_198253.2		upstream	C228T	c.−124C>T	Pathogenic	38	12	26	31.58
	6							Deletion							
	10							Deletion							
	7				EGFR			Amplification							
	9				CDKN2A			Loss							
	9				CDKN2B			Loss							
	10				PTEN			Loss							
12	1	65306996	GT	G	JAK1	NM_002227.4	19	frame_shift	p.Lys860fs	c.2580delA	Pathogenic	1016	76	940	7.48
	1	120491681	CTT	C	NOTCH2	NM_024408.4	16	frame_shift	p.Lys849fs	c.2546_2547delAA	Pathogenic	1468	57	1411	3.88
	3	37053589	C	T	MLH1	NM_000249.3	8	stop_gained+splice_site_region	p.Arg226*	c.676C>T	Pathogenic	645	575	70	89.15
	3	47155365	C	A	SETD2	NM_014159.6	5	splice_site_donor+intron	splicing	c.4715+1G>T	Pathogenic	718	559	159	77.86

	4	55133559	A	G	PDGFRA	NM_006206.6	6	non_synonymous_coding	p.Tyr288Cys	c.863A>G	Pathogenic	1477	567	910	38.39
	9	139413069	TAGA	T	NOTCH1	NM_017617.5	6	codon_change_plus_codon_deletion	p.Phe357del	c.1070_1072delTCT	Pathogenic	1166	51	1115	4.37
	10	89717712	C	T	PTEN	NM_000314.8	7	non_synonymous_coding	p.Pro246Leu	c.737C>T	Pathogenic	1702	543	1159	31.90
	10	89720852	C	T	PTEN	NM_000314.8	8	stop_gained	p.Arg335*	c.1003C>T	Pathogenic	842	183	659	21.73
	11	108128334	G	A	ATM	NM_000051.3	15	splice_site_donor+intron	splicing	c.2376+1G>A	Pathogenic	643	63	580	9.80
	17	7572962	GT	G	TP53	NM_000546.5	11	frame_shift	p.Lys382fs	c.1146delA	Pathogenic	1347	461	886	34.22
	17	7577121	G	A	TP53	NM_000546.5	8	non_synonymous_coding	p.Arg273Cys	c.817C>T	Pathogenic	1080	37	1043	3.43
	17	7577548	C	T	TP53	NM_000546.5	7	non_synonymous_coding	p.Gly245Ser	c.733G>A	Pathogenic	1188	327	861	27.53
	17	7577551	C	A	TP53	NM_000546.5	7	non_synonymous_coding	p.Gly244Cys	c.730G>T	Pathogenic	1193	46	1147	3.86
	17	29667571	C	T	NF1	NM_000267.3	46	stop_gained	p.Gln2303*	c.6907C>T	Pathogenic	1211	339	872	27.99
13	3	37056000	C	T	MLH1	NM_000249.3	9	Non_synonymous_coding	p.Ser252Leu	c.755C>T	Pathogenic	483	218	265	45.13
	12	49434991	G	A	KMT2D	NM_003482.3	31	Non_synonymous_coding	p.Arg2188Cys	c.6562C>T	Pathogenic	61	26	35	42.62
	17	7577094	G	A	TP53	NM_000546.5	8	Non_synonymous_coding	p.Arg282Trp	c.844C>T	Pathogenic	511	82	429	16.05
	17	7579494	T	A	TP53	NM_000546.5	4	Stop_gained	p.Arg65*	c.193A>T	Pathogenic	293	56	237	19.11
	19	4090601	C	T	MAP2K2	NM_030662.3	11	Non_synonymous_coding	p.Val400Met	c.1198G>A	Pathogenic	56	28	28	50.00
	7				EGFR			Amplification							
14	1	11181421	G	T	MTOR	NM_004958.3	49	non_synonymous_coding	p.Ala2272Asp	c.6815C>A	Pathogenic	1031	390	641	37.83
	1	39889724	C	T	MACF1	NM_012090.5	55	stop_gained	p.Arg3330*	c.9988C>T	Pathogenic	403	113	290	28.04
	1	120460307	C	T	NOTCH2	NM_024408.3	33	non_synonymous_coding	p.Arg2003Gln	c.6008G>A	Pathogenic	1441	553	888	38.38
	1	120506308	C	T	NOTCH2	NM_024408.3	11	non_synonymous_coding	p.Ala602Thr	c.1804G>A	Pathogenic	1875	289	1586	15.41
	2	162273096	A	G	TBR1	NM_006593.2	1	non_synonymous_coding	p.Met59Val	c.175A>G	Pathogenic	1352	607	745	44.90

	2	190717474	C	T	PMS1	NM_000534.4	7	stop_gained	p.Arg265*	c.793C>T	Pathogenic	271	94	177	34.69
	2	215610467	A	AT	BARD1	NM_000465.3	8	frame_shift	p.Tyr597fs	c.1788dupA	Pathogenic	1363	502	861	36.83
	3	37058999	C	T	MLH1	NM_000249.3	10	non_synonymous_coding+splice_site_region	p.Arg265Cys	c.793C>T	Pathogenic	912	370	542	40.57
	3	47098735	C	A	SETD2	NM_014159.6	15	non_synonymous_coding	p.Ser2180Ile	c.6539G>T	Pathogenic	2582	324	2258	12.55
	3	47098949	G	A	SETD2	NM_014159.6	15	stop_gained	p.Arg2109*	c.6325C>T	Pathogenic	979	423	556	43.21
	3	101038520	C	T	IMPG2	NM_016247.3	2	non_synonymous_coding	p.Arg81Lys	c.242G>A	Pathogenic	1811	688	1123	37.99
	3	121206428	C	T	POLQ	NM_199420.3	16	non_synonymous_coding	p.Asp1784Asn	c.5350G>A	Pathogenic	1375	489	886	35.56
	3	121207695	C	A	POLQ	NM_199420.3	16	non_synonymous_coding	p.Gln1361His	c.4083G>T	Pathogenic	2979	1267	1712	42.53
	3	178916876	G	A	PIK3CA	NM_006218.2	2	non_synonymous_coding	p.Arg88Gln	c.263G>A	Pathogenic	708	32	676	4.52
	4	55152112	C	A	PDGFRA	NM_006206.4	18	non_synonymous_coding	p.Asn848Lys	c.2544C>A	Pathogenic	1853	767	1086	41.39
	4	187629400	C	T	FAT1	NM_005245.3	2	non_synonymous_coding	p.Glu528Lys	c.1582G>A	Pathogenic	2276	911	1365	40.03
	4	187629475	C	T	FAT1	NM_005245.3	2	non_synonymous_coding	p.Ala503Thr	c.1507G>A	Pathogenic	2155	841	1314	39.03
	4	187630604	A	AT	FAT1	NM_005245.3	2	frame_shift	p.Asn126fs	c.377dupA	Pathogenic	1646	646	1000	39.25
	5	112175639	C	T	APC	NM_000038.5	16	stop_gained	p.Arg1450*	c.4348C>T	Pathogenic	742	179	563	24.12
	6	135522778	T	C	MYB	NM_001130173.1	14	non_synonymous_coding+splice_site_region	p.Val651Ala	c.1952T>C	Pathogenic	1242	128	1114	10.31
	7	6031649	G	A	PMS2	NM_000535.5	9	stop_gained	p.Arg315*	c.943C>T	Pathogenic	402	154	248	38.31
	7	6043355	G	A	PMS2	NM_000535.5	4	non_synonymous_coding	p.Arg107Trp	c.319C>T	Pathogenic	670	233	437	34.78
	7	55249088	G	A	EGFR	NM_005228.3	20	non_synonymous_coding	p.Gly796Ser	c.2386G>A	Pathogenic	2177	240	1937	11.02
	7	148543575	C	T	EZH2	NM_004456.4	3	non_synonymous_coding	p.Arg78His	c.233G>A	Pathogenic	940	336	604	35.74
	7	155604800	C	A	SHH	NM_000193.3	1	non_synonymous_coding	p.Arg6Ile	c.17G>T	Pathogenic	2325	1063	1262	45.72
	8	26221271	A	AT	PPP2R2A	NM_001177591.1	8	frame_shift	p.Ser292fs	c.874dupT	Pathogenic	1025	353	672	34.44

	9	2086873	G	T	SMARCA2	NM_001289396.1	18	non_synonymous_coding	p.Lys857Asn	c.2571G>T	Pathogenic	852	347	505	40.73
	9	2115850	G	A	SMARCA2	NM_001289396.1	25	non_synonymous_coding	p.Arg1162His	c.3485G>A	Pathogenic	1099	493	606	44.86
	9	98239828	C	T	PTCH1	NM_000264.3	10	splice_site_donor+intron	splicing	c.1503+1G>A	Pathogenic	943	321	622	34.04
	11	65422181	G	A	RELA	NM_021975.3	11	stop_gained	p.Gln442*	c.1324C>T	Pathogenic	855	378	477	44.21
	11	108216611	C	T	ATM	NM_000051.3	58	non_synonymous_coding	p.Arg2854Cys	c.8560C>T	Pathogenic	1003	298	705	29.71
	12	5021064	G	A	KCNA1	NM_000217.2	2	non_synonymous_coding	p.Val174Ile	c.520G>A	Pathogenic	1585	618	967	38.99
	12	57496280	C	T	STAT6	NM_001178078.1	12	splice_site_acceptor+intron	splicing	c.1306−1G>A	Pathogenic	1712	684	1028	39.95
	12	112926872	C	T	PTPN11	NM_002834.3	13	non_synonymous_coding	p.Arg498Trp	c.1492C>T	Pathogenic	1673	685	988	40.94
	12	133202355	T	C	POLE	NM_006231.3	47	non_synonymous_coding+splice_site_region	p.Asp2178Gly	c.6533A>G	Pathogenic	989	324	665	32.76
	14	95557411	G	A	DICER1	NM_030621.4	28	stop_gained	p.Arg1855*	c.5563C>T	Pathogenic	533	155	378	29.08
	16	2114342	C	T	TSC2	NM_000548.3	15	stop_gained	p.Arg505*	c.1513C>T	Pathogenic	773	247	526	31.95
	16	2125862	G	A	TSC2	NM_000548.3	23	non_synonymous_coding	p.Ala870Thr	c.2608G>A	Pathogenic	1651	97	1554	5.88
	17	7577022	G	A	TP53	NM_000546.5	8	stop_gained	p.Arg306*	c.916C>T	Pathogenic	2536	966	1570	38.09
	19	1221986	C	T	STK11	NM_000455.4	7	non_synonymous_coding	p.Arg301Trp	c.901C>T	Pathogenic	930	110	820	11.83
	19	15291812	C	T	NOTCH3	NM_000435.2	18	non_synonymous_coding	p.Arg985His	c.2954G>A	Pathogenic	824	339	485	41.14
	19	50921136	C	T	POLD1	NM_002691.3	27	non_synonymous_coding	p.Arg1086Trp	c.3256C>T	Pathogenic	802	350	452	43.64
	20	57484851	G	A	GNAS	NM_000516.5	10	stop_gained	p.Trp277*	c.831G>A	Pathogenic	1638	632	1006	38.58
	22	24176329	C	T	SMARCB1	NM_003073.3	9	non_synonymous_coding+splice_site_region	p.Arg374Trp	c.1120C>T	Pathogenic	574	42	532	7.32
	22	30067911	G	T	NF2	NM_000268.3	11	stop_gained	p.Glu366*	c.1096G>T	Pathogenic	1144	418	726	36.54
	X	53223614	G	A	KDM5C	NM_004187.3	23	non_synonymous_coding	p.Arg1249Cys	c.3745C>T	Pathogenic	1265	43	1222	3.40
	X	53241007	C	A	KDM5C	NM_004187.3	9	non_synonymous_coding	p.Asp402Tyr	c.1204G>T	Pathogenic	1204	158	1046	13.12

	X	70465638	C	A	ZMYM3	NM_005096.3	17	stop_gained	p.Glu914*	c.2740G>T	Pathogenic	1337	646	691	48.32
	X	76937799	C	CT	ATRX	NM_000489.4	9	frame_shift	p.Gln984fs	c.2948dupA	Pathogenic	525	153	372	29.14
	X	76944355	C	CT	ATRX	NM_000489.4	7	frame_shift	p.Asp184fs	c.549dupA	Pathogenic	740	327	413	44.19
15	1	97547924	C	A	DPYD	NM_000110.3	22	Non_synonymous_coding	p.Gly957Cys	c.2869G>T	Pathogenic	3915	134	3781	3.42
	3	37056035	C	A	MLH1	NM_000249.3	9	Non_synonymous_coding +splice_site_region	p.His264Asn	c.790C>A	Pathogenic	2692	158	2534	5.87
	7	128829018	G	C	SMO	NM_005631.4	1	Non_synonymous_coding	p.Gly9Ala	c.26G>C	Pathogenic	91	31	60	34.07
	10	89720852	C	T	PTEN	NM_001304717.2	9	Stop_gained	p.Arg508*	c.1522C>T	Pathogenic	2862	1828	1034	63.87
	17	29657343	T	A	NF1	NM_001042492.2	39	Stop_gained	p.Leu1880*	c.5639T>A	Pathogenic	2063	112	1951	5.43
	17	41258531	G	A	BRCA1	NM_007300.3	4	Non_synonymous_coding	p.Leu52Phe	c.154C>T	Pathogenic	1281	159	1122	12.41
	19	11098500	G	A	SMARCA4	NM_001128849.1	6	Non_synonymous_coding	p.Ala340Thr	c.1018G>A	Pathogenic	485	419	66	86.39
	9				CDKN2B			Loss							
16	3	37042521	T	G	MLH1	NM_000249.3	3	Non_synonymous_coding	p.Ser95Ala	c.283T>G	Pathogenic	1160	620	540	53.45
	4	55131142	G	A	PDGFRA	NM_006206.4	5	Non_synonymous_coding	p.Glu229Lys	c.685G>A	Pathogenic	27101	25627	1474	94.56
	4	55564586	G	C	KIT	NM_000222.2	3	Non_synonymous_coding	p.Lys158Asn	c.474G>C	Pathogenic	2398	632	1775	25.98
	5	1295228	G	A	TERT	NM_198253.2		Upstream	C228T	c.−124C>T	Pathogenic	79	29	50	36.71
	10	89717734	C	CA	PTEN	NM_001304717.2	8	Frame_shift	p.Val428fs	c.1281dupA	Pathogenic	1742	1087	655	62.40
	19	42777194	A	C	CIC	NM_001304815.1	2	Non_synonymous_coding	p.Gln420Pro	c.1259A>C	Pathogenic	462	54	408	11.69
	4				PDGFRA			Amplification							
	9				CDKN2A			Deletion							
	9				CDKN2B			Deletion							
	10				PTEN			Loss							

	X				STAG2			Loss							
17	7	92404146	C	A	CDK6	NM_001145306.1	2	SPLICE_SITE_ACCEPTOR+INTRON	splicing	c.234−1G>T	Pathogenic	910	50	860	5.0
	1	72400995	C	A	NEGR1	NM_173808.2	1	SPLICE_SITE_ACCEPTOR+INTRON	splicing	c.177−1G>T	Pathogenic	870	61	809	7.0
	4				KIT			Amplification							
	3	37045965	G	T	MLH1	NM_000249.3	4	NON_SYNONYMOUS_CODING+ SPLICE_SITE_REGION	p.Arg127Ile	c.380G>T	Pathogenic	778	42	736	5.0
	17	29528178	G	T	NF1	NM_001042492.2	10	SPLICE_SITE_DONOR+INTRON	splicing	c.1185+1G>T	Pathogenic	614	105	509	17.0
	17	29585450	C	A	NF1	NM_001042492.2	32	NON_SYNONYMOUS_CODING	p.Pro1421Gln	c.4262C>A	Likely Pathogenic	818	44	774	5.0
	4				PDGFRA			Amplification							
	17	7577539	G	A	TP53	NM_000546.5	7	NON_SYNONYMOUS_CODING	p.Arg248Trp	c.742C>T	Pathogenic	576	37	539	6.0
	17	7578413	C	A	TP53	NM_000546.5	5	NON_SYNONYMOUS_CODING	p.Val173Leu	c.517G>T	Pathogenic	359	30	329	8.0
18	10				PTEN			Loss							
	12				CDK4			Amplification							
	1	2.26E+08	A	T	H3F3A	NM_002107.4	2	Non_synonymous_coding	p.Lys28Met	c.83A>T	Pathogenic	1462	659	803	45.08
	3	37067145	TG	T	MLH1	NM_000249.3	12	Frame_shift	p.Ala353fs	c.1057delG	Likely Pathogenic	910	494	416	54.29
	17	7577120	C	T	TP53	NM_001126112.2	8	Non_synonymous_coding	p.Arg273His	c.818G>A	Pathogenic	1018	966	52	94.89
19	X	76919003	CTT	CA	ATRX	NM_000489.4	12	Frame_shift+non_synonymous_coding	p.Glu1329fs	c.3986_3987delAAinsT	Likely Pathogenic	827	734	93	88.75
	X	44949074	A	G	KDM6A	NM_001291415.1	26	Non_synonymous_coding	p.Gln1264Arg	c.3791A>G	Likely Pathogenic	2237	336	1901	15.02
	1	11259759	C	T	MTOR	NM_004958.3	27	Non_synonymous_coding+splice_site_region	p.Asp1316Asn	c.3946G>A	Likely Pathogenic	3149	707	2442	22.45
	2	2.09E+08	C	T	IDH1	NM_001282386.1	4	Non_synonymous_coding	p.Arg132His	c.395G>A	Pathogenic	3634	1708	1926	47.0
	9	2076229	G	A	SMARCA2	NM_001289396.1	13	Non_synonymous_coding+splice_site_region	p.Asp646Asn	c.1936G>A	Likely Pathogenic	1892	646	1246	34.14

	9				CDKN2A/2B			Homozygous deletion							
	3	37090464	C	T	MLH1	NM_000249.3	18	Non_synonymous_coding	p.Arg687Trp	c.2059C>T	Pathogenic	1929	1680	249	87.09
	17	29486068	C	T	NF1	NM_001042492.2	3	Non_synonymous_coding	p.Ser82Phe	c.245C>T	Likely Pathogenic	3592	597	2995	16.62
	17	29533275	G	A	NF1	NM_001042492.2	12	Stop_gained	p.Trp426*	c.1278G>A	Pathogenic	4759	1090	3669	22.9
	17	29588828	G	A	NF1	NM_001042492.2	35	Stop_gained	p.Trp1559*	c.4677G>A	Pathogenic	4937	890	4047	18.03
	17	29664601	G	A	NF1	NM_001042492.2	43	Splice_site_donor+intron	splicing	c.6642+1G>A	Pathogenic	2099	482	1617	22.96
	17	7577539	G	C	TP53	NM_000546.5	7	Non_synonymous_coding	p.Arg248Gly	c.742C>G	Pathogenic	923	885	38	95.88
20	X	39916407	C	A	BCOR	NM_001123385.1	11	SPLICE_SITE_DONOR+INTRON	splicing	c.4595+1G>T	Pathogenic	487	409	78	84.0
	9	1.39E+08	G	A	NOTCH1	NM_017617.3	3	STOP_GAINED	p.Arg56*	c.166C>T	Pathogenic	149	60	89	40.0
	19	15290015	C	T	NOTCH3	NM_000435.2	22	NON_SYNONYMOUS_CODING	p.Gly1180Asp	c.3539G>A	Likely Pathogenic	389	172	217	44.0
	3	47165282	C	CT	SETD2	NM_014159.6	3	FRAME_SHIFT	p.Glu282fs	c.843dupA	Likely Pathogenic	637	248	389	39.0
	2	48032123	T	TA	MSH6	NM_000179.2	6	FRAME_SHIFT	p.Arg1172fs	c.3514dupA	Pathogenic	615	495	120	80.0
	2	2.09E+08	C	T	IDH1	NM_001282386.1	4	NON_SYNONYMOUS_CODING	p.Arg132His	c.395G>A	Pathogenic	1230	464	766	38.0
	17	29486049	G	GA	NF1	NM_001042492.2	3	FRAME_SHIFT	p.Asn78fs	c.233dupA	Likely Pathogenic	623	243	380	39.0
	17	29665110	C	T	NF1	NM_001042492.2	45	STOP_GAINED	p.Arg2258*	c.6772C>T	Pathogenic	1613	665	948	41.0
	17	7574003	G	A	TP53	NM_000546.5	10	STOP_GAINED	p.Arg342*	c.1024C>T	Pathogenic	1061	450	611	42.0
	17	7577121	G	A	TP53	NM_000546.5	8	NON_SYNONYMOUS_CODING	p.Arg273Cys	c.817C>T	Pathogenic	1190	485	705	41.0
21	2	48033352	C	T	MSH6	NM_000179.2	8	non_synonymous_coding	p.Thr1219Ile	c.3656C>T	Pathogenic	315	16	299	5.08
	2	48033420	C	T	MSH6	NM_000179.2	8	non_synonymous_coding	p.Arg1242Cys	c.3724C>T	Pathogenic	459	21	438	4.58
	2	121729593	C	T	GLI2	NM_005270.4	7	non_synonymous_coding	p.Thr379Ile	c.1136C>T	Pathogenic	1168	300	868	25.68
	2	209113112	C	T	IDH1	NM_005896.3	4	non_synonymous_coding	p.Arg132His	c.395G>A	Pathogenic	941	310	631	32.94

	17	7578394	T	C	TP53	NM_000546.5	5	non_synonymous_coding	p.His179Arg	c.536A>G	Pathogenic	1838	1674	164	91.08
	X	76855027	CCT	C	ATRX	NM_000489.4	25	frame_shift	p.Lys1936fs	c.5807_5808delAG	Pathogenic	150	141	9	94.00
	17p							Deletion							
	22q							Deletion							
	4				PDGFRA			Amplification							
	4				KIT			Amplification							
	9				CDKN2A			Deletion							
	9				CDKN2B			Deletion							
22	6	117662349	C	G	ROS1	NM_002944.2	30	Non_synonymous_coding	p.Trp1676Cys	c.5028G>C	Pathogenic	1342	629	713	46.87
	7	6031630	A	G	PMS2	NM_000535.5	9	Non_synonymous_coding	p.Val321Ala	c.962T>C	Pathogenic	956	137	819	14.33
	14	95570219	G	A	DICER1	NM_001271282.2	21	Non_synonymous_coding	p.Leu1172Phe	c.3514C>T	Pathogenic	3084	1121	1963	36.35
	14	95570220	A	C	DICER1	NM_001271282.2	21	Non_synonymous_coding	p.Asp1171Glu	c.3513T>G	Pathogenic	3124	1151	1973	36.84
	X	76912052	T	TGTTCTGGG	ATRX	NM_000489.4	13	Frame_shift	p.Arg1405fs	c.4204_4211dupCCCAGAAC	Pathogenic	250	74	176	29.60
	9				CDKN2A			Loss							
	9				CDKN2B			Loss							
	22				MN1			Loss							
	22				EWSR1			Loss							
	22				NF2			Loss							
23	1	51439637	C	T	CDKN2C	NM_001262.2	3	Stop_gained	p.Arg68*	c.202C>T	Pathogenic	1605	343	1562	18.01

	2	29473981	C	T	ALK	NM_004304.4	12	Non_synonymous_coding	p.Asp732Asn	c.2194G>A	Pathogenic	582	62	520	10.65
	2	48010479	C	T	MSH6	NM_000179.2	1	Non_synonymous_coding	p.Ala36Val	c.107C>T	Pathogenic	487	217	270	44.56
	2	209113112	C	T	IDH1	NM_001282386.1	4	Non_synonymous_coding	p.Arg132His	c.395G>A	Pathogenic	1927	611	1316	31.71
	3	178948044	A	G	PIK3CA	NM_006218.2	20	Non_synonymous_coding	p.Asp939Gly	c.2816A>G	Pathogenic	552	274	278	49.64
	5	1295228	G	A	TERT	NM_198253.2		Upstream	C228T	c.−124C>T	Pathogenic	346	115	231	33.24
	5	79950705	GGCTGCAGCGGCCGCAGCGG	GC	MSH3	NM_002439.4	1	Non_synonymous_coding+codon_change_plus_codon_deletio	p.Ala54_Ala60delinsPro	c.160_178delGCTGCAGCGGCCGCAGCGGinsC	Pathogenic	567	199	368	35.10
	8	67488596	C	G	MYBL1	NM_001080416.3	10	Non_synonymous_coding	p.Trp372Cys	c.1116G>C	Pathogenic	1180	587	593	49.75
	17	7577153	C	T	TP53	NM_000546.5	8	Non_synonymous_coding+splice_site_region	p.Gly262Asp	c.785G>A	Pathogenic	1997	85	1912	4.26
	19	42793244	T	G	CIC	NM_001304815.1	8	Splice_site_donor+intron	splicing	c.3861+2T>G	Pathogenic	298	39	259	13.09
24	3	37067242	C	T	MLH1	NM_000249.3	12	Non_synonymous_coding	p.Arg385Cys	c.1153C>T	Pathogenic	1097	522	575	47.58
	4	175899037	T	A	ADAM29	NM_001130703.1	4	Non_synonymous_coding	p.His787Gln	c.2361T>A	Pathogenic	1035	91	944	8.79
	10	104268924	A	G	SUFU	NM_016169.3	1	Splice_site_acceptor+intron	splicing	c.183−2A>G	Pathogenic	854	823	31	96.37
25	2	48033790	G	A	MSH6	NM_000179.2	9	non_synonymous_coding+splice_site_region	p.Arg1334Gln	c.4001G>A	Pathogenic	158	87	71	55.06
	7	140453136	A	T	BRAF	NM_004333.4	15	non_synonymous_coding	p.Val600Glu	c.1799T>A	Pathogenic	715	217	498	30.35
	17	7578212	G	A	TP53	NM_000546.5	6	stop_gained	p.Arg213*	c.637C>T	Pathogenic	1083	80	1003	7.39
	9				CDKN2A			Loss							
	9				CDKN2B			Loss							

	9				NOTCH1			Loss							

c, chrmosome number; E, exon number; Ref, reference; Alt, alteration; Ref seq, reference sequence; pos, position number

Table 5. The list of the FIRST brain tumor panel established by the Department of Pathology, Seoul National University Hospital (FIRST means Friendly, Integrated, Research-based, Smart and Trustworthy).

Brain tumor panel													
DNA												RNA	
ACVR1	BARD1	C11ORF95	DAXX	EGFR	FAM175A	GABRA5	H2AFX	IDH1	JAK1	KBTBD4	MAB21L2	ALK	NTRK2
ADAM29	BCL3	CBL	DDX3X	EMX2	FANCA	GAD1	H3F3A	IDH2	JUN	KCNA1	MACF1	AXL	NTRK3
ADGRB3	BCOR	CCND1	DICER1	EOMES	FANCD2	GFI1	HHIP	IMPG2		KDM5C	MAP2K1	BCOR	NUTM1
ADGRG4	BRAF	CCND2	DIDO1	EPHA7	FANCL	GFI1B	HIST1H3B			KDM6A	MAP2K2	BRAF	PCSK5
AIP	BRCA1	CCND3	DKK2	ERBB2	FAT1	GLI1	HIST1H3C			KHDRBS2	MAPK1	C11ORF95	PDGFRA
AKAP6	BRCA2	CD300C	DPYD	ERCC2	FBXW7	GLI2	HRAS			KIT	MAPK3	CIC	PDGFRB
AKT1	BRIP1	CD79A		ERG	FGF3	GNAS				KLF4	MDM2	DDIT3	PIK3CA
ALK		CDH1		ETV6	FGF4	GPR101				KMT2C	MDM4	DDX31	PKD1
APC		CDK12		EWSR1	FGF6	GSE1				KMT2D	MED12	EGFR	PPARG
ARID1A		CDK4		EYA1	FGFR1					KRAS	MEN1	ERBB4	PRKCA
ARID1B		CDK6		EZH2	FGFR2						MET	ERG	PVT1

ARID2		CDKN1A			FGFR3						MLH1
ATM		CDKN1B			FGFR4						MLH3
ATOH1		CDKN2A			FLG						MN1
ATRX		CDKN2B			FUBP1						MRE11A
		CDKN2C									MSH2
		CHEK1									MSH3
		CHEK2									MSH4
		CIC									MSH5
		CREBBP									MSH6
		CSNK2B									MTOR
		CTDNEP1									MYB
		CTNNB1									MYBL1
											MYC
											MYCN
											MYL1
NEGR1	OTX2	PALB2	RAD51B	SETD2	TBR1	UNC5D	VHL	WIF1	YAP1	ZIC1	
NF1		PDGFRA	RAD51C	SFRP1	TCF4	USP8				ZMYM3	
NF2		PDGFRB	RAD51D	SHH	TERT						

ETV1	RAF1
ETV4	RELA
EWSR1	RET
FGFR1	ROS1
FGFR2	SLC44A1
FGFR3	SS18
FOXO1	STAT6
FOXR2	TAF15
FUS	TFE3
GFI1	TGFBR3
GFI1B	TTYH1
HMGA2	WHSC1
MET	YAP1
MN1	
MYB	
NRG1	
NTRK1	

NOTCH1		PDZD2	RAD54L	SMAD2	TNC						
NOTCH2		PIK3CA	RB1	SMAD4	TP53						
NOTCH3		PMS1	RBM24	SMARCA2	TRAF7						
NPR3		PMS2	RELA	SMARCA4	TSC1						
NRAS		POLD1	RET	SMARCB1	TSC2						
NRL		POLE	RGPD3	SMARCE1							
NTRK1		POLQ	ROS1	SMO							
NTRK2		PPM1D		SSTR2							
NTRK3		PPP2R2A		STAG2							
		PRDM6		STAT3							
		PRKAR1A		STAT6							
		PRKCA		STK11							
		PTCH1		SUFU							
		PTCH2		SYNCRIP							
		PTEN									
		PTPN11									

Table 6. Primer sequences used for Sanger germline sequencing.

Primers	Primer Sequences (5' → 3')
MLH1 exon 4 (F)	GTGCTCATCGTTGCCACATA
MLH1 exon 4 (R)	CGTACTCAAGATCTCTGCCAAA
MLH1 exon 18 (F)	CGCCTAAAGTATCACATTTCGTT
MLH1 exon 18 (R)	GATGGGCAAGTTTCATCTCC
MSH2 exon 10 (F)	ATCCATCCTCAGGTGCTCAT
MSH2 exon 10 (R)	TGCGACAGCTGACTGCTCTA
MSH6 exon 4 (F1)	CTGGAAGGTGATCCCTCTGA
MSH6 exon 4 (R1)	CCTTTAAGCACCTGGGGTAA
MSH6 exon 4 (F2)	GTGCCCCACTCTGTAACCAT
MSH6 exon 4 (R2)	CAGGAAAACGACCTTCAGGA
MSH6 exon 5 (F)	GGAGATCGTTGGACTGTAATTGA
MSH6 exon 5 (R)	TCCTCTTCCTCACAGCCTATTA
MSH6 exon 9 (F)	ACCCCAGCCAGGAGACTATT
MSH6 exon 9 (R)	TCATAGTGCATCATCCCTTCC

Table 7. The list of pathogenic and likely pathogenic mutations found in the initial brain tumors of Case 10, Case 17 and Case 19 through NGS studies with a comprehensive brain tumor-targeted gene panel.

Case	Chr	Pos	Ref	Alt	Gene	Refseq	Exon	Effect	AA	CDS	Pathogenic	Read	Alt	Ref	Vaf (%)
10	5	1295228	G	A	TERT	NM_198253.2		upstream	C228T	c.-124C>T	Pathogenic	48	18	30	37.50
	10	89720785	CAAGG	C	PTEN	NM_000314.6	8	frame_shift	p.Lys313fs	c.939_942delGGAA	Pathogenic	37	27	10	72.97
	17	7578212	G	A	TP53	NM_000546.5	6	stop_gained	p.Arg213*	c.637C>T	Pathogenic	480	200	280	41.67
	17	7578437	G	A	TP53	NM_000546.5	5	stop_gained	p.Gln165*	c.493C>T	Pathogenic	1930	805	1125	41.71
	7				EGFR			Amplification							
	10				PTEN			Loss							
	12				GLI1			Amplification							
	12				CDK4			Amplification							
17	2	227661044	G	A	IRS1	NM_005544.2	1	Non_synonymous_coding	p.Ala804Val	c.2411C>T	Pathogenic	2217	1046	1171	47.18
	7	55272966	G	A	EGFR	NM_005228.3	28	Non_synonymous_coding	p.Val1097Ile	c.3289G>A	Pathogenic	4006	1874	2132	46.78
	10	89720648	TA	TTT	PTEN	NM_001304717.2	8	Splice_site_acceptor+intron	splicing	c.1321-2delAinsTT	Pathogenic	1015	158	857	15.57
	17	29528178	G	T	NF1	NM_001042492.2	10	Splice_site_donor+intron	splicing	c.1185+1G>T	Pathogenic	3568	1174	2394	32.90
	9				CDKN2A			Loss							
	9				CDKN2B			Loss							
	17				TP53			Loss							
	17				ERBB2			Loss							
19	1	97981298	G	A	DPYD	NM_000110.3	13	Non_synonymous_coding	p.Thr575Ile	c.1724C>T	Pathogenic	1190	69	1121	5.80

	2	209113112	C	T	IDH1	NM_005896.3	4	Non_synonymous_coding	p.Arg132His	c.395G>A	Pathogenic	2521	1144	1377	45.38
	10	43604541	G	A	RET	NM_020975.4	6	Non_synonymous_coding	p.Val376Ile	c.1126G>A	Pathogenic	1170	62	1108	5.30
	10	89711876	G	A	PTEN	NM_000314.4	6	Non_synonymous_coding	p.Gly165Glu	c.494G>A	Pathogenic	1133	87	1046	7.68
	15	90628282	G	A	IDH2	NM_002168.3	9	Non_synonymous_coding	p.Arg377Cys	c.1129C>T	Pathogenic	737	79	658	10.72
	17	7577539	G	C	TP53	NM_001126112.2	7	Non_synonymous_coding	p.Arg248Gly	c.742C>G	Pathogenic	603	554	49	91.87
	17	7578492	C	T	TP53	NM_001126112.2	5	Stop_gained	p.Trp146*	c.438G>A	Pathogenic	644	62	582	9.63
	17	41209140	C	T	BRCA1	NM_007300.3	20	Non_synonymous_coding	p.Val1757Ile	c.5269G>A	Pathogenic	1003	63	940	6.28
	19	15302426	G	A	NOTCH3	NM_000435.2	6	Non_synonymous_coding	p.Pro282Leu	c.845C>T	Pathogenic	1701	155	1546	9.11
	3				MLH1			Deletion			Pathogenic				
	5				PIK3R1			Loss			Pathogenic				
	8				MYC			Gain			Pathogenic				
	9				CDKN2A			Deletion			Pathogenic				
	9				CDKN2B			Deletion			Pathogenic				
	10				PTEN			Loss			Pathogenic				

Table 8. The comparison of clinicopathological and molecular features of Lynch syndrome−associated MMRD brain tumors and Sporadic MMRD brain tumors

	Lynch syndrome−associated MMRD brain tumors (n=4)	Sporadic MMRD brain tumors (n=21)
Age (year)	35−75 (median : 60)	1−78 (median : 46)
Sex (M : F)	1 : 3	2 : 1
Location	supratentorial area	supratentorial and infratentorial area
Histologic feature		
Giant cell	100% (4/4)	71% (15/21)
MVP	75% (3/4)	90% (19/21)
necrosis	75% (3/4)	81% (17/21)
Tumor type	GBM IDH−wt (3/4) PXA (1/4)	GBM IDH−wt (including 1 Gliosarcoma) (14/21) DMG H3 K27M−m (1/21) Astrocytoma, IDH−m (3/21) Anaplastic meningioma (1/21) Oligodendroglioma (1/21) Medulloblastoma (1/21)
MMR gene mutation	MSH2 (1/4) MSH6 (3/4)	MLH1 (10/21) PMS2 (2/21) MSH2 (3/21) MSH6 (5/21) MLH1/PMS2 (1/21)
MSI−H	75% (100% of HGG)	33%
MGMT methylation	50%	53%

Acknowledgments

This study was supported by a grant from the Korea Health Technology R&D Project through the Korea Health Industry Development Institute (KHIDI), funded by the Ministry of Health & Welfare, Republic of Korea (grant number: HI14C1277).

Competing interests

The authors declare no competing interests.

Ethics approval and consent to participate

The institutional review board of our hospital approved this study (IRB No: 1906-020-1037), which has therefore been performed under the ethical standards set out in the 1964 Declaration of Helsinki and its subsequent amendments. As this study is a retrospective review of anonymized electronic medical records, pathology data, and NGS data derived from a brain tumor-specific somatic gene panel, informed consent was waived by our IRB under the Korean Bioethics and Safety Act.

Bibliography

1. Friedberg, E.C., et al., *DNA repair and mutagenesis*. 2005: American Society for Microbiology Press.
2. Li, G.-M., *Mechanisms and functions of DNA mismatch repair.* Cell research, 2008. **18**(1): p. 85-98.
3. Iyer, R.R., et al., *DNA mismatch repair: functions and mechanisms.* Chemical reviews, 2006. **106**(2): p. 302-323.
4. Jascur, T. and C.R. Boland, *Structure and function of the components of the human DNA mismatch repair system.* International Journal of Cancer, 2006. **119**(9): p. 2030-2035.
5. Jiricny, J., *The multifaceted mismatch-repair system.* Nature reviews Molecular cell biology, 2006. **7**(5): p. 335-346.
6. Jun, S.H., T.G. Kim, and C. Ban, *DNA mismatch repair system: Classical and fresh roles.* The FEBS journal, 2006. **273**(8): p. 1609-1619.
7. Pećina-Šlaus, N., et al., *Mismatch repair pathway, genome stability and cancer.* Frontiers in molecular biosciences, 2020: p. 122.
8. Harfe, B.D., B.K. Minesinger, and S. Jinks-Robertson, *Discrete in vivo roles for the MutL homologs Mlh2p and Mlh3p in the removal of frameshift intermediates in budding yeast.* Current Biology, 2000. **10**(3): p. 145-148.
9. Huang, Y. and G.-M. Li, *DNA mismatch repair in the context of chromatin.* Cell & bioscience, 2020. **10**(1): p. 1-8.
10. Reyes, G.X., et al., *New insights into the mechanism of DNA mismatch repair.* Chromosoma, 2015. **124**(4): p. 443-462.
11. Brown, M.W., et al., *Dynamic DNA binding licenses a repair factor to*

bypass roadblocks in search of DNA lesions. Nature Communications, 2016. **7**(1): p. 1-12.

12. Fishel, R., *Mismatch repair.* Journal of Biological Chemistry, 2015. **290**(44): p. 26395-26403.
13. Jiricny, J., *Postreplicative mismatch repair.* Cold Spring Harbor perspectives in biology, 2013. **5**(4): p. a012633.
14. Edelbrock, M.A., S. Kaliyaperumal, and K.J. Williams, *Structural, molecular and cellular functions of MSH2 and MSH6 during DNA mismatch repair, damage signaling and other noncanonical activities.* Mutation Research/Fundamental and Molecular Mechanisms of Mutagenesis, 2013. **743**: p. 53-66.
15. Liu, D., G. Keijzers, and L.J. Rasmussen, *DNA mismatch repair and its many roles in eukaryotic cells.* Mutation Research/Reviews in Mutation Research, 2017. **773**: p. 174-187.
16. Kadyrov, F.A., et al., *Endonucleolytic function of MutLα in human mismatch repair.* cell, 2006. **126**(2): p. 297-308.
17. Cannavo, E., et al., *Characterization of the interactome of the human MutL homologues MLH1, PMS1, and PMS2.* Journal of Biological Chemistry, 2007. **282**(5): p. 2976-2986.
18. Prindle, M.J. and L.A. Loeb, *DNA polymerase delta in DNA replication and genome maintenance.* Environmental and molecular mutagenesis, 2012. **53**(9): p. 666-682.
19. Itkonen, H.M., et al., *Human DNA polymerase α interacts with mismatch repair proteins MSH 2 and MSH 6.* FEBS letters, 2016. **590**(23): p. 4233-4241.
20. Shimodaira, H., et al., *Interaction of mismatch repair protein PMS2 and the p53-related transcription factor p73 in apoptosis response to cisplatin.* Proceedings of the National Academy of Sciences, 2003.

100(5): p. 2420-2425.

21. Kasela, M., M. Nyström, and M. Kansikas, *PMS2 expression decrease causes severe problems in mismatch repair.* Human mutation, 2019. 40(7): p. 904-907.

22. Modrich, P. and R. Lahue, *Mismatch repair in replication fidelity, genetic recombination, and cancer biology.* Annual review of biochemistry, 1996. 65(1): p. 101-133.

23. Kolodner, R., *Biochemistry and genetics of eukaryotic mismatch repair.* Genes & development, 1996. 10(12): p. 1433-1442.

24. Pope, B.J., et al., *Germline and tumor sequencing as a diagnostic tool to resolve suspected Lynch syndrome.* The Journal of Molecular Diagnostics, 2021. 23(3): p. 358-371.

25. Ionov, Y., et al., *Ubiquitous somatic mutations in simple repeated sequences reveal a new mechanism for colonic carcinogenesis.* Nature, 1993. 363(6429): p. 558-561.

26. Loeb, L.A., *Mutator phenotype may be required for multistage carcinogenesis.* Cancer research, 1991. 51(12): p. 3075-3079.

27. Shibata, D., et al., *Genomic instability in repeated sequences is an early somatic event in colorectal tumorigenesis that persists after transformation.* Nature genetics, 1994. 6(3): p. 273-281.

28. Zhang, H., et al., *Apoptosis induced by overexpression of hMSH2 or hMLH1.* Cancer Research, 1999. 59(13): p. 3021-3027.

29. Schmidt, M.H. and C.E. Pearson, *Disease-associated repeat instability and mismatch repair.* DNA repair, 2016. 38: p. 117-126.

30. Dietmaier, W., et al., *Diagnostic microsatellite instability: definition and correlation with mismatch repair protein expression.* Cancer research, 1997. 57(21): p. 4749-4756.

31. Boland, C.R., et al., *A National Cancer Institute Workshop on*

Microsatellite Instability for cancer detection and familial predisposition: development of international criteria for the determination of microsatellite instability in colorectal cancer. Cancer research, 1998. **58**(22): p. 5248-5257.

32. Frayling, I., *Microsatellite instability.* Gut, 1999. **45**(1): p. 1-4.

33. Bocker, T., et al., *Microsatellite instability analysis: a multicenter study for reliability and quality control.* Cancer Research, 1997. **57**(21): p. 4739-4743.

34. Wang, L., et al., *Tumor mutational burden is associated with poor outcomes in diffuse glioma.* BMC cancer, 2020. **20**(1): p. 1-12.

35. Daniel, P., et al., *Temozolomide induced hypermutation in glioma: evolutionary mechanisms and therapeutic opportunities.* Frontiers in oncology, 2019. **9**: p. 41.

36. Lombardi, G., et al., *Pembrolizumab activity in recurrent high-grade gliomas with partial or complete loss of mismatch repair protein expression: A monocentric, observational and prospective pilot study.* Cancers, 2020. **12**(8): p. 2283.

37. Caccese, M., et al., *Mismatch-repair protein expression in high-grade gliomas: a large retrospective multicenter study.* International journal of molecular sciences, 2020. **21**(18): p. 6716.

38. Biller, L.H., S. Syngal, and M.B. Yurgelun, *Recent advances in Lynch syndrome.* Familial Cancer, 2019. **18**(2): p. 211-219.

39. WARTHIN, A.S., *Heredity with reference to carcinoma: as shown by the study of the cases examined in the pathological laboratory of the University of Michigan, 1895-1913.* Archives of internal medicine, 1913. **12**(5): p. 546-555.

40. Boland, C.R., *Evolution of the nomenclature for the hereditary colorectal cancer syndromes.* Familial cancer, 2005. **4**(3): p. 211-

218.

41. Guerrini-Rousseau, L., et al., *Constitutional mismatch repair deficiency-associated brain tumors: report from the European C4CMMRD consortium.* Neuro-oncology advances, 2019. **1**(1): p. vdz033.

42. Moreira, L., et al., *Identification of Lynch syndrome among patients with colorectal cancer.* Jama, 2012. **308**(15): p. 1555-1565.

43. Bhattacharya, P. and T.W. McHugh, *Lynch syndrome*, in *StatPearls [Internet]*. 2021, StatPearls Publishing.

44. Aarnio, M., et al., *Cancer risk in mutation carriers of DNA-mismatch-repair genes.* International journal of cancer, 1999. **81**(2): p. 214-218.

45. Barrow, E., et al., *Cumulative lifetime incidence of extracolonic cancers in Lynch syndrome: a report of 121 families with proven mutations.* Clinical genetics, 2009. **75**(2): p. 141-149.

46. Vasen, H., et al., *The risk of brain tumours in hereditary non-polyposis colorectal cancer (HNPCC).* International Journal of Cancer, 1996. **65**(4): p. 422-425.

47. Watson, P., et al., *The risk of extra-colonic, extra-endometrial cancer in the Lynch syndrome.* International journal of cancer, 2008. **123**(2): p. 444-449.

48. Shia, J., *Immunohistochemistry versus microsatellite instability testing for screening colorectal cancer patients at risk for hereditary nonpolyposis colorectal cancer syndrome: part I. The utility of immunohistochemistry.* The Journal of molecular diagnostics, 2008. **10**(4): p. 293-300.

49. Weissman, S.M., et al., *Genetic counseling considerations in the evaluation of families for Lynch syndrome—a review.* Journal of

genetic counseling, 2011. **20**(1): p. 5-19.

50. Latham, A., et al., *Microsatellite instability is associated with the presence of Lynch syndrome pan-cancer.* Journal of clinical oncology, 2019. **37**(4): p. 286.

51. Brahmer, J., et al., *Nivolumab versus docetaxel in advanced squamous-cell non-small-cell lung cancer.* New England Journal of Medicine, 2015. **373**(2): p. 123-135.

52. Robert, C., et al., *Ipilimumab plus dacarbazine for previously untreated metastatic melanoma.* New England Journal of Medicine, 2011. **364**(26): p. 2517-2526.

53. Apolo, A.B., et al., *Avelumab, an anti-programmed death-ligand 1 antibody, in patients with refractory metastatic urothelial carcinoma: results from a multicenter, phase ib study.* Journal of Clinical Oncology, 2017. **35**(19): p. 2117.

54. Powles, T., et al., *MPDL3280A (anti-PD-L1) treatment leads to clinical activity in metastatic bladder cancer.* Nature, 2014. **515**(7528): p. 558-562.

55. Ansell, S.M., et al., *PD-1 blockade with nivolumab in relapsed or refractory Hodgkin's lymphoma.* New England Journal of Medicine, 2015. **372**(4): p. 311-319.

56. Kaufman, H.L., et al., *Avelumab in patients with chemotherapy-refractory metastatic Merkel cell carcinoma: a multicentre, single-group, open-label, phase 2 trial.* The lancet oncology, 2016. **17**(10): p. 1374-1385.

57. Yi, M., et al., *Biomarkers for predicting efficacy of PD-1/PD-L1 inhibitors.* Molecular cancer, 2018. **17**(1): p. 1-14.

58. Lemery, S., P. Keegan, and R. Pazdur, *First FDA approval agnostic of cancer site-when a biomarker defines the indication.* The New

England journal of medicine, 2017. **377**(15): p. 1409-1412.

59. Zhao, P., et al., *Mismatch repair deficiency/microsatellite instability-high as a predictor for anti-PD-1/PD-L1 immunotherapy efficacy.* Journal of hematology & oncology, 2019. **12**(1): p. 1-14.

60. Chan, T.A., et al., *Development of tumor mutation burden as an immunotherapy biomarker: utility for the oncology clinic.* Annals of Oncology, 2019. **30**(1): p. 44-56.

61. McGranahan, T., et al., *Current state of immunotherapy for treatment of glioblastoma.* Current treatment options in oncology, 2019. **20**(3): p. 1-15.

62. Thorsson, V., et al., *The immune landscape of cancer.* Immunity, 2018. **48**(4): p. 812-830. e14.

63. Medikonda, R., et al., *A review of glioblastoma immunotherapy.* Journal of neuro-oncology, 2021. **151**(1): p. 41-53.

64. Hodges, T.R., et al., *Mutational burden, immune checkpoint expression, and mismatch repair in glioma: implications for immune checkpoint immunotherapy.* Neuro-oncology, 2017. **19**(8): p. 1047-1057.

65. Bouffet, E., et al., *Immune checkpoint inhibition for hypermutant glioblastoma multiforme resulting from germline biallelic mismatch repair deficiency.* Journal of clinical oncology, 2016. **34**(19): p. 2206-2211.

66. Johanns, T.M., et al., *Immunogenomics of hypermutated glioblastoma: a patient with germline POLE deficiency treated with checkpoint blockade immunotherapy.* Cancer discovery, 2016. **6**(11): p. 1230-1236.

67. Indraccolo, S., et al., *Genetic, epigenetic, and immunologic profiling of MMR-deficient relapsed glioblastoma.* Clinical Cancer Research,

2019. **25**(6): p. 1828-1837.

68. Martinez, R., et al., *Low-level microsatellite instability phenotype in sporadic glioblastoma multiforme.* Journal of cancer research and clinical oncology, 2005. **131**(2): p. 87-93.

69. Albayrak, A., et al., *Clinical pan-cancer assessment of mismatch repair deficiency using Tumor-Only, targeted next-generation sequencing.* JCO Precision Oncology, 2020. **4**: p. 1084-1097.

70. Cho, Y.A., et al., *Incidence, clinicopathologic, and genetic characteristics of mismatch repair gene-mutated glioblastomas.* Journal of neuro-oncology, 2021. **153**(1): p. 43-53.

71. Umar, A., et al., *Revised Bethesda Guidelines for hereditary nonpolyposis colorectal cancer (Lynch syndrome) and microsatellite instability.* Journal of the National Cancer Institute, 2004. **96**(4): p. 261-268.

72. Graham, R.P., et al., *Heterogenous MSH6 loss is a result of microsatellite instability within MSH6 and occurs in sporadic and hereditary colorectal and endometrial carcinomas.* The American journal of surgical pathology, 2015. **39**(10): p. 1370-1376.

73. Chen, W. and W.L. Frankel, *A practical guide to biomarkers for the evaluation of colorectal cancer.* Modern Pathology, 2019. **32**(1): p. 1-15.

74. Louis, D.N., et al., *The 2021 WHO classification of tumors of the central nervous system: a summary.* Neuro-oncology, 2021. **23**(8): p. 1231-1251.

75. Louis, D.N., et al., *cIMPACT-NOW update 6: new entity and diagnostic principle recommendations of the cIMPACT-Utrecht meeting on future CNS tumor classification and grading*. 2020, Wiley Online Library.

76. Benjamin, D., et al., *Calling somatic SNVs and indels with Mutect2.* BioRxiv, 2019: p. 861054.

77. Karczewski, K.J., et al., *The mutational constraint spectrum quantified from variation in 141,456 humans.* Nature, 2020. **581**(7809): p. 434-443.

78. Wang, K., M. Li, and H. Hakonarson, *ANNOVAR: functional annotation of genetic variants from high-throughput sequencing data.* Nucleic acids research, 2010. **38**(16): p. e164-e164.

79. Untergasser, A., et al., *Primer3—new capabilities and interfaces.* Nucleic acids research, 2012. **40**(15): p. e115-e115.

80. Gu, Z., R. Eils, and M. Schlesner, *Complex heatmaps reveal patterns and correlations in multidimensional genomic data.* Bioinformatics, 2016. **32**(18): p. 2847-2849.

81. De Lellis, L., et al., *Integrative analysis of hereditary nonpolyposis colorectal cancer: the contribution of allele-specific expression and other assays to diagnostic algorithms.* PloS one, 2013. **8**(11): p. e81194.

82. Therkildsen, C., et al., *Glioblastomas, astrocytomas and oligodendrogliomas linked to Lynch syndrome.* European journal of neurology, 2015. **22**(4): p. 717-724.

83. Azam, S., et al., *Lynch Syndrome With Germline MSH2 Mutation in a Patient With Primary Anaplastic Glioneuronal Tumor.* JCO Precision Oncology, 2019. **3**: p. 1-6.

84. Suwala, A.K., et al., *Primary mismatch repair deficient IDH-mutant astrocytoma (PMMRDIA) is a distinct type with a poor prognosis.* Acta neuropathologica, 2021. **141**(1): p. 85-100.

85. Amayiri, N., et al., *High frequency of mismatch repair deficiency among pediatric high grade gliomas in J ordan.* International journal

of cancer, 2016. **138**(2): p. 380-385.

86. Lorans, M., et al., *Update on hereditary colorectal cancer: improving the clinical utility of multigene panel testing.* Clinical colorectal cancer, 2018. **17**(2): p. e293-e305.

87. Shirts, B.H., et al., *Using somatic mutations from tumors to classify variants in mismatch repair genes.* The American Journal of Human Genetics, 2018. **103**(1): p. 19-29.

88. Leung, S.Y., et al., *Chromosomal instability and p53 inactivation are required for genesis of glioblastoma but not for colorectal cancer in patients with germline mismatch repair gene mutation.* Oncogene, 2000. **19**(35): p. 4079-4083.

89. Brat, D.J., et al., *cIMPACT-NOW update 3: recommended diagnostic criteria for "Diffuse astrocytic glioma, IDH-wildtype, with molecular features of glioblastoma, WHO grade IV".* Acta neuropathologica, 2018. **136**(5): p. 805-810.

90. Lowder, L., et al., *Gliosarcoma: distinct molecular pathways and genomic alterations identified by DNA copy number/SNP microarray analysis.* Journal of Neuro-oncology, 2019. **143**(3): p. 381-392.

91. Wang, Y., et al., *Clinical features and molecular markers on diffuse midline gliomas with H3K27M mutations: A 43 cases retrospective cohort study.* Frontiers in oncology, 2021. **10**: p. 3353.

92. Brat, D.J., et al., *cIMPACT-NOW update 5: recommended grading criteria and terminologies for IDH-mutant astrocytomas.* Acta neuropathologica, 2020. **139**(3): p. 603-608.

93. Cimino, P.J., *Malignant progression to anaplastic meningioma: neuropathology, molecular pathology, and experimental models.* Experimental and molecular pathology, 2015. **99**(2): p. 354-359.

94. Rahner, N. and V. Steinke, *Hereditary cancer syndromes.* Deutsches

Ärzteblatt International, 2008. **105**(41): p. 706.

95. Lynch, H.T., et al., *Predominance of brain tumors in an extended Li-Fraumeni (SBLA) kindred, including a case of Sturge-Weber syndrome.* Cancer: Interdisciplinary International Journal of the American Cancer Society, 2000. **88**(2): p. 433-439.

96. Choi, S., et al., *Temozolomide-associated hypermutation in gliomas.* Neuro-oncology, 2018. **20**(10): p. 1300-1309.

97. Wojciechowicz, K., et al., *Temozolomide increases the number of mismatch repair-deficient intestinal crypts and accelerates tumorigenesis in a mouse model of Lynch syndrome.* Gastroenterology, 2014. **147**(5): p. 1064-1072. e5.

98. Kawaguchi, K., et al., *Genetic Characteristics of Mismatch Repair-deficient Glioblastoma.* NMC Case Report Journal, 2021. **8**(1): p. 565-571.

99. Higuchi, F., et al., *Restoration of temozolomide sensitivity by PARP inhibitors in mismatch repair deficient glioblastoma is independent of base excision repair.* Clinical Cancer Research, 2020. **26**(7): p. 1690-1699.

100. Giunti, L., et al., *Type A microsatellite instability in pediatric gliomas as an indicator of Turcot syndrome.* European journal of human genetics, 2009. **17**(7): p. 919-927.

101. Alonso, M., et al., *Microsatellite instability occurs in distinct subtypes of pediatric but not adult central nervous system tumors.* Cancer research, 2001. **61**(5): p. 2124-2128.

102. Gylling, A., et al., *Differential cancer predisposition in Lynch syndrome: insights from molecular analysis of brain and urinary tract tumors.* Carcinogenesis, 2008. **29**(7): p. 1351-1359.

103. Hegi, M.E., et al., *MGMT gene silencing and benefit from*

temozolomide in glioblastoma. New England Journal of Medicine, 2005. **352**(10): p. 997-1003.

104. Weisenberger, D.J., *Characterizing DNA methylation alterations from the cancer genome atlas.* The Journal of clinical investigation, 2014. **124**(1): p. 17-23.

105. Donson, A.M., et al., *MGMT promoter methylation correlates with survival benefit and sensitivity to temozolomide in pediatric glioblastoma.* Pediatric blood & cancer, 2007. **48**(4): p. 403-407.

106. Dodgshun, A.J., et al., *Germline-driven replication repair-deficient high-grade gliomas exhibit unique hypomethylation patterns.* Acta neuropathologica, 2020. **140**(5): p. 765-776.

107. Maxwell, J.A., et al., *Mismatch repair deficiency does not mediate clinical resistance to temozolomide in malignant glioma.* Clinical Cancer Research, 2008. **14**(15): p. 4859-4868.

108. Goenka, A., et al., *The many facets of therapy resistance and tumor recurrence in glioblastoma.* Cells, 2021. **10**(3): p. 484.

Abstract in Korean

요약 (국문초록)

산발성 불일치 복구 유전자 결핍 뇌종양 및 린치 증후군 관련 불일치 복구 유전자 결핍 뇌종양

김 현 희

의학과 병리학 전공

서울대학교 대학원

불일치 복구 유전자 결핍 뇌종양은 원발성 뇌종양 중에서 드물며, 불일치 복구 유전자의 생식세포 돌연변이 또는 산발적 돌연변이에 의해 유도된다.

본 연구에서는 불일치 복구 유전자 결핍 뇌종양의 임상병리학적 및 분자유전학적 특성과 생물학적 행동을 알기 위해 25례의 (산발적 뇌종양 21례 및 린치 증후군 연관 뇌종양 4례) 원발성 불일치 복구 유전자 결핍 뇌종양을 연구 및 보고한다. 25례의 불일치 복구 유전자 결핍 뇌종양에는 1례의 신경교육종을 포함하는 IDH-야생형 교모세포종 17례, IDH-돌연변이형 CNS WHO 4등급의 성상세포종 3례, H3 K27M-

돌연변이를 동반한 미만성 정중선 신경교종 1례, 역형성 수막종 1례, IDH 돌연변이 및 염색체 1번의 단완과 염색체 19번의 장완의 동반 결손이 있는 희소돌기신경교종 1례, SHH 활성화 및 TP53-야생형 CNS WHO 4등급인 광범위한 결절이 있는 수모세포종 1례, 다형성 황색성상세포종 1례가 포함되었다.

본 연구에서는 불일치 복구 유전자 결핍 뇌종양에 대한 뇌종양 표적 유전자 패널을 이용한 차세대 염기서열분석, 현미부수체 불안정성 검사, 불일치 복구 유전자의 생식세포 돌연변이 검출을 위한 Sanger 염기서열분석, 불일치 복구 단백질 관련 면역조직화학염색검사, 임상병리학적 분석 및 생존분석을 수행했다.

본 연구의 증례 중 84%에서 종양세포의 돌연변이 수가 높게 관찰되었고, 나머지 증례인 IDH-야생형 교모세포종, 미만성 정중선 신경교종, 수모세포종 및 다형성 황색성상세포종 각 1례에서 낮은 종양세포의 돌연변이 수 (단일염기다형성 수가 5개 보다 적음)가 관찰되었다. MLH1, MSH6, MSH2 및 PMS2 돌연변이는 각각 40%, 32%, 16% 및 8%에서 발견되었다. MLH1과 PMS2 돌연변이가 함께 관찰되는 환자가 1례 (4%) 있었다. 고빈도 현미부수체 불안정형과 저빈도 현미부수체 불안정형은 각각 41%와 18%에서 발견되었고, 나머지 41%는 현미부수체 안정형이었다. 모든 린치 증후군 연관 교모세포종은 고빈도 현미부수체 불안정형이었다. 또한, 총 증례의 76%(19/25)는 조직병리학적으로 다핵 거대 세포가 관찰되었다. 동시항암화학방사선치료와 테모졸로마이드 치료를 받은 MGMT 프로모터 메틸화가 있는 뇌종양일 때 무진행 생존 기간은 불일치 복구 유전자 결핍이 있는 뇌종양 환자가 불일치 복구 유전자 결핍이 없는 뇌종양 환자보다 긴 경향이 있었지만 생존 분석을 시행한 환자의 수가 적고, 추적관찰 기간이 짧아 의미있는 결과를 얻기에는 충분하지 않았다.

본 연구를 통해 그동안 드물게 연구된 불일치 복구 유전자 결핍 뇌종양의 임상병리학적, 분자유전학적인 특성을 알 수 있었다. 특히 불일치 복구 유전자 결핍을 동반한 미만성 정중선 신경교종과 역형성 수막종의 특성 및 MSH2 p.Tyr405* 체세포 돌연변이는 이전에 보고가 없었던 것으로 새로운 발견이다.

주요어 : 불일치 복구 유전자, 린치 증후군, 현미부수체 불안정성, 종양 돌연변이 부하, 교모세포종, 유전성 암 증후군

학 번 : 2018-32894